ΜΕΤΑΠΤΥΧΙΑΚΗ ΔΙΠΛΩΜΑΤΙΚΗ ΕΡΓΑΣΙΑ

Φορετά συστήματα, πολυλειτουργικά υλικά και εύκαμπτες δομές

Μεταπτυχιακός Φοιτητής: Αριστείδης Ρεπούλιας, ΑΜ 0014
Επιβλέπων: Σάββας Βασιλειάδης, Καθηγητής

ΑΙΓΑΛΕΩ, 24 Φεβρουαρίου 2020

ΠΑΝΕΠΙΣΤΗΜΙΟ ΔΥΤΙΚΗΣ ΑΤΤΙΚΗΣ
ΣΧΟΛΗ ΜΗΧΑΝΙΚΩΝ
Τμήμα Ηλεκτρολόγων & Ηλεκτρονικών Μηχανικών
www.eee.uniwa.gr
Θηβών 250, Αθήνα-Αιγάλεω 12244
Τηλ. +30 210 538-1225, Fax. +30 210 538-1226

Πρόγραμμα Μεταπτυχιακών Σπουδών
Ηλεκτρικές & Ηλεκτρονικές Επιστήμες μέσω Έρευνας

UNIVERSITY of WEST ATTICA
FACULTY OF ENGINEERING
Department of Electrical & Electronics
Engineering
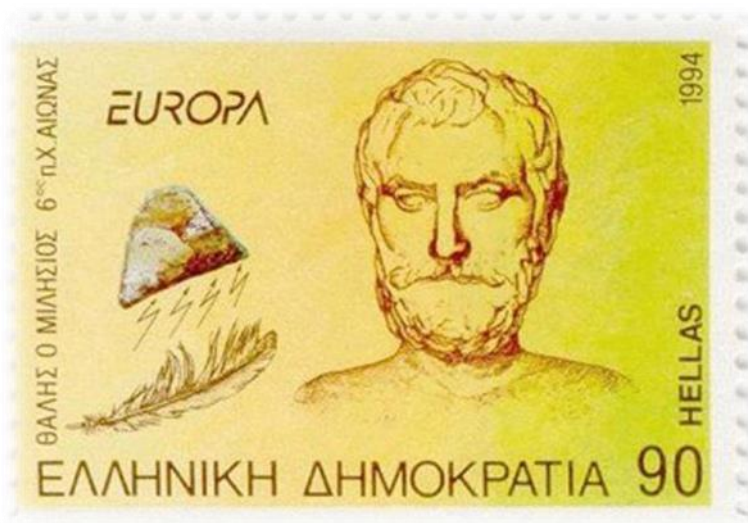www.eee.uniwa.gr
250, Thivon Str., Athens, GR-12244, Greece
Tel:+30 210 538-1225, Fax:+30 210 538-1226

Master of Science By Research in
Electrical & Electronics Engineering

MSc Thesis

Wearable systems, multifunctional materials and flexible structures

Student: Aristeidis Repoulias, Registration Number 0014
MSc Thesis Supervisor: Savvas Vasiliadis, Professor

ATHENS-EGALEO, 24th February 2020

Μεταπτυχιακή Διπλωματική Εργασία, Αριστείδης Ρεπούλιας, ΑΜ 0014

Η Μεταπτυχιακή Διπλωματική Εργασία έγινε αποδεκτή, εξετάστηκε και βαθμολογήθηκε από την εξής τριμελή εξεταστική επιτροπή:

Επιβλέπων	Μέλος	Μέλος
ΣΑΒΒΑΣ ΒΑΣΙΛΕΙΑΔΗΣ	ΓΕΩΡΓΙΟΣ ΠΑΤΣΗΣ	ΣΟΦΙΑ ΚΑΛΟΓΕΡΟΠΟΥΛΟΥ
Καθηγητής	Καθηγητής	Καθηγήτρια

Μεταπτυχιακή Διπλωματική Εργασία, Αριστείδης Ρεπούλιας, ΑΜ 0014

ΔΗΛΩΣΗ ΣΥΓΓΡΑΦΕΑ
ΜΕΤΑΠΤΥΧΙΑΚΗΣ ΔΙΠΛΩΜΑΤΙΚΗΣ ΕΡΓΑΣΙΑΣ

Ο κάτωθι υπογεγραμμένος Αριστείδης Ρεπούλιας του Αλεξάνδρου, με αριθμό μητρώου 0014 φοιτητής του Προγράμματος Μεταπτυχιακών Σπουδών «Ηλεκτρικές & Ηλεκτρονικές Επιστήμες μέσω Έρευνας», του Τμήματος Ηλεκτρολόγων και Ηλεκτρονικών Μηχανικών, της Σχολής Μηχανικών του Πανεπιστημίου Δυτικής Αττικής, δηλώνω ότι:

«Είμαι ο συγγραφέας αυτής της μεταπτυχιακής διπλωματικής εργασίας και κάθε βοήθεια την οποία είχα για την προετοιμασία της, είναι πλήρως αναγνωρισμένη και αναφέρεται στην εργασία. Επίσης, οι όποιες πηγές από τις οποίες έκανα χρήση δεδομένων, ιδεών ή λέξεων, είτε ακριβώς είτε παραφρασμένες, αναφέρονται στο σύνολό τους, με πλήρη αναφορά στους συγγραφείς, τον εκδοτικό οίκο ή το περιοδικό, συμπεριλαμβανομένων και των πηγών που ενδεχομένως χρησιμοποιήθηκαν από το διαδίκτυο. Επίσης, βεβαιώνω ότι αυτή η εργασία έχει συγγραφεί από μένα αποκλειστικά και αποτελεί προϊόν πνευματικής ιδιοκτησίας τόσο δικής μου, όσο και του Ιδρύματος.

Παράβαση της ανωτέρω ακαδημαϊκής μου ευθύνης αποτελεί ουσιώδη λόγο για την ανάκληση του τίτλου μου».

Ο Δηλών

Αριστείδης Ρεπούλιας
Μεταπτυχιακός Φοιτητής

SUMMARY

Triboelectricity is a natural phenomenon, which had been considered to cause only negative results until some years ago. Wide research has been applied over the last decade to use it positively, mainly in energy harvesting and monitoring sensors. But most of the interest has focused on its novel applications than on how it exactly works.

The integration of textiles in these novel applications makes them more promising as they can provide large surface areas and continuous activation thanks to the lasting movement of the wearer, while on the other hand, they can offer flexibility, elasticity, breathability, robustness etc to the final product. No matter if their electric outputs are lower than the ones of complicated materials and sophisticated structures, they can be used efficiently in signal sensoring or low energy demanding electronic parts.

The understanding of how textile structures can perform in the triboelectric phenomenon is the foundation to develop their efficiency. This raises an interest due to the special characteristics of textiles, in a period that a lot of research is applied on the development of light, flexible and wearable triboelectric generators used for energy harvesting or self-powered sensors.

But parameters related to the electrical outcomes of the textile structures, like the contact time duration of the fabrics, the force applied between the fabrics, the effective contact depending on the direction and orientation of the fabrics surfaces and the structure's surface pattern has not been studied thoroughly. Thus it would be necessary to reproduce the phenomenon in a real environment under controllable conditions and make the appropriate tests.

Considering all the above facts, plus the absence of a standard method to be used for the study or comparison of the triboelectric behaviour of textile structures, the need for building a prototype testing device has risen. This was designed and developed based on the vertical contact-separation mode, to allow us to measure different samples under the same conditions or the same sample under different conditions.

Textile fabric samples were paired and tested. A small similarity on the voltages was noticed between reverse orientations of the samples surfaces, meaning between 0° and 180°, and between -90° and 90°, which might be caused by the different surface contact of the paired fabrics due to the warps and wefts presence. Moreover, an increase of the voltage values with the increase of the contact force between the textile fabric samples surfaces was found, when using certain samples which give significant electric outputs. It was also previewed that the contact duration does not affect the selected samples output voltage and that the surface pattern of a textile fabric can be of major importance for its triboelectric outcomes.

KEYWORDS: textile, fabric, material, triboelectricity, triboelectric generator, testing device, contact-separation mode.

ΠΕΡΙΛΗΨΗ

Ο τριβοηλεκτρισμός είναι ένα φυσικό φαινόμενο, το οποίο μέχρι πριν μερικά χρόνια θεωρούνταν ότι προκαλεί μόνο προβλήματα. Αντίθετα την τελευταία δεκαετία έχει προσεγγισθεί θετικά και ερευνάται ευρέως, κυρίως σε δομές γεννητριών τριβοηλεκτρικής ενέργειας και αυτοτροφοδοτούμενων αισθητήρων. Ωστόσο το μεγαλύτερο μέρος της διεθνούς έρευνας έχει επικεντρωθεί στις καινοτόμες εφαρμογές του και στον επίτευξη όλο και πιο μεγάλων παραγώμενων τάσεων παρά στο πώς λειτουργεί ακριβώς.

Η ενσωμάτωση των κλωστοϋφαντουργικών δομών σε αυτές τις νέες εφαρμογές, τις βελτιώνει κατα πολύ καθώς μπορούν να διαθέτουν πιο μεγάλες επιφάνειες (αύξηση απόδοσης) και να παραμένουν σε διαρκή ενεργοποίηση χάρη πχ στη διαρκή κίνηση του χρήστη (βιωσημότητα). Επιπλέον μπορούν να προσφέρουν στο τελικό προϊόν ευελιξία, ελαστικότητα, διαπνοή, αντοχή κ.λ.π. Τα κλωστοϋφαντουργικά υλικά αν και δίνουν χαμηλές τιμές τάσης και ρεύματος σε σχέση με πιο εξελιγμένα υλικά, παρόλα αυτά μπορούν να χρησιμοποιηθούν αποτελεσματικά σε αισθητήρια ή σε ηλεκτρονικά εξαρτήματα που απαιτούν χαμηλή κατανάλωση ενέργειας.

Η κατανόηση της συμπεριφοράς των κλωστοϋφαντουργικών δομών κατα τον τριβοηλεκτρισμό, είναι θεμελιώδης για την ανάπτυξη της αποτελεσματικότητάς τους.

Όμως δεν έχουν μελετηθεί διεξοδικά οι παράμετροι που μπορούν να επηρεάσουν την παραγώμενη τάση των κλωστοϋφαντουργικών δομών, όπως πχ η διάρκεια επαφής των υφασμάτων, η δύναμη που εφαρμόζεται μεταξύ τους, ο προσανατολισμός τους κατα την επαφή, η μορφή της επιφάνειας τους κλπ.

Λαμβάνοντας υπόψη όλες τις παραπάνω τάσεις εξέλιξης και τα κενά μελέτης, καθώς και την απουσία μιας τυποποιημένης μεθόδου για να χρησιμοποιηθεί στη μελέτη ή στη σύγκριση της τριβοηλεκτρικής συμπεριφοράς των κλωστοϋφαντουργικών δομών, οδηγηθήκαμε στην απόφαση της κατασκευής μιας πρότυπης συσκευής ελέγχου του τριβοηλεκτρισμού για κλωστοϋφαντουργικές δομές. Αυτή σχεδιάστηκε και αναπτύχθηκε στηριζόμενη στην αρχή της κατακόρυφης επαφής και του κατακόρυφου διαχωρισμού των δυο υπο εξέταση επιφανειών.

Τέλος δοκίμια υφασμάτων συνδυάστηκαν και μετρήθηκαν. Μία μικρή ομοιότητα στις τάσεις παρατηρήθηκε κατα την περιστροφή κάποιων δοκιμίων σε συγκεκριμμένες γωνίες. Επιπλέον, διαπιστώθηκε αύξηση των τιμών τάσης με την αύξηση της δύναμης επαφής μεταξύ των επιφανειών των δοκιμίων. Η διάρκεια επαφής τους φάνηκε να μην επηρεάζει την παραγώμενη τάση, ενώ τέλος η μορφή δομής της επιφάνειας τους φάνηκε να επηρεάζει σημαντικά τη παραγώμενη τάση.

ΛΕΞΕΙΣ ΚΛΕΙΔΙΑ: ύφασμα, κλωστοϋφαντουργική δομή, κλωστοϋφαντουργικό υλικό, υλικό, τριβοηλεκτρισμός, τριβοηλεκτρική γεννήτρια, συσκευή μέτρησης.

ACKNOWLEDGEMENT

I would like to express my deepest appreciation to the Professor Savvas Vasiliadis for his contribution in this thesis, and his valuable support into my effort to broaden my horizons into new scientific areas.

ΕΥΧΑΡΙΣΤΙΕΣ

Θα ήθελα να εκφράσω την εκτίμησή μου και να ευχαριστήσω τον Καθηγητή Σάββα Βασιλειάδη για τη συνεισφορά του σε αυτή τη διπλωματική εργασία, και την πολύτιμη υποστήριξή του στο να ανοίξω τους ορίζοντες μου σε νέες επιστιμονικές περιοχές.

Μεταπτυχιακή Διπλωματική Εργασία, Αριστείδης Ρεπούλιας, ΑΜ 0014

TABLE OF CONTENTS

SUMMARY + KEYWORDS

TABLE OF CONTENTS

INTRODUCTION: Subject, research questions and structure of the work

CHAPTER I: Theoretical context of the subject - Field overview

Μεταπτυχιακή Διπλωματική Εργασία, Αριστείδης Ρεπούλιας, ΑΜ 0014

CHAPTER II: Research methodology

CHAPTER III: The method – Justification, Design, Development

CHAPTER IV: Experiment and Results

CHAPTER V: Analysis of Results – Discussion

CHAPTER VI: Conclusions

BIBLIOGRAPHY – SOURCES

INTRODUCTION:
Subject, research questions and structure of the work

Although triboelectricity is familiar in our lives, a big part it is remaining unknown as for the actual mechanisms and reasons it happens [1]. One of the reasons for this is that most researches focus only on creating new triboelectricity based developments, regardless of understanding how and why it occurs, as long as this doesn't seem to be required necessarily to achieve the previous goal [1].

Moreover, measuring the charge exchange after contact of two materials involves a large number of variables like the lack of precision, surface impurities, charge backflow on separation, ambient conditions, material transfer from one surface to another etc. All of these can impact the measurements and some of them are not understood or easily controlled, thus making the whole scientific approach of triboelectricity to be done slowly and under difficulties all this time [2].

But since the electrical charge coming from triboelectricity is low, and since the miniaturized and low consumption portable electrical devices are becoming more and more popular, there has arisen a high interest for scientists to apply it on wearable electronics [3]. The idea of powering small, portable, ultralow-power consumption electronic devices which are worldwide used (e.g. smartphones or smart watches) by harvesting energy from our everyday activities sounds challenging [3].

The integration of textiles in this process makes it more promising as these can have large surface areas and continuous activation thanks to the lasting movement of the wearer. There are numerous textile specifications which can differentiate a textile structure (e.g. material composition, weaving or knitting pattern, thickness, density, roughness etc). Keeping in mind that different textiles structures can be combined together too, then their contribution in triboelectricity and in the wearable applications becomes very interesting.

To achieve this goal, a standard method or a testing device is needed to properly study and compare these fabric structures, achieve the creation of desired electrical output demands and apply them on wearable electronics. But currently, because of the difficulties for an overall explanation of the triboelectricity mechanism and the forthcoming spread of wearable electronics, most of the scientific articles focus on new promising triboelectricity based developments, of increasing electrical outputs, complicated structures and state of the art materials. Only a few of these articles examine how certain parameters (e.g. contact frequency, material's thickness, contact force etc) affect the electrical outputs of the published structures.

Keeping in mind the before mentioned problem which prevents comparisons of materials or structures under same conditions, the recent increasing interest on the triboelectricity phenomenon, plus the multidisciplinary nature of textile materials, this research focused on building a testing device with controllable behaviour which can be used to compare the electrical outputs of textile fabrics.

In this study, the first chapter introduces the triboelectricity phenomenon, in four sections. The first section offers the definition, quick historical reference, advantages and disadvantages, plus the relation to textiles. The second section presents the fundamental theory, paradoxes, charge transfer mechanisms and more. The third section focuses on the charge generators based on triboelectricity, their history, operation modes, advantages, combinations, structure examples, textile-based examples, efficiency parameters and application examples. The forth section gets into the issues and obstacles which applications practically face.

The second chapter presents the methodology which will be used, the target of the tests, the software and hardware demands, plus the necessity of using a generic measuring device to study the phenomenon or compare fabric samples.

The third chapter refers to the design and development of the suggested method which will be used to approach and examine the phenomenon, and describes the necessary demands of the device which will be built, plus the parameters which may affect its proper operation.

The fourth chapter refers to the application details of the tests and their results in details. The fifth chapter analyses and discusses the results of the current experimental part. Finally in the sixth chapter are presented the conclusions of the use of the proposed device and a reference to future work.

1. Introduction

1.1. Definition of triboelectricity

Triboelectricity is defined as the phenomenon where electrical charges are generated between two materials when we bring them in contact, we separate them or rub them [4]. Its intensity relates to the electron affinities on their surfaces [4] and external factors [3]. The charges of the two materials are opposite in sign but equal in magnitude [3]. The two materials can be different or even seemingly chemically identical [2].

1.2. Historical reference about triboelectricity

The Greek philosopher, mathematician, and astronomer Thales of Miletus, who lived from 624-623 BC to 548-545 BC, is historically known as the one who discovered the phenomenon of triboelectricity. What he noticed exactly, was the charging effect caused when rubbing amber and wool together [1]. Moreover, the term triboelectricity comes from the ancient Greek words "tribe" which means to rub and "electro" which means amber, thus meaning "rubbing amber" [1].

It is important to mention that although in the past the triboelectric phenomenon used to be simply related on friction, on recent years researchers have tumbled this belief according to Molnar et al., and proved that the contact of the materials is the real reason [3].

Another simplifying assumption made in the past was that in a given pair of contact charging materials, one would charge uniformly positively and the other uniformly negatively. But later in 2011 Baytekin et al. showed that the previous simplified assumption is not right, and a totally different mechanism was happening on the material's surface [5].

So, considering triboelectricity as a physics phenomenon, in the beginning, only physics was trying to find out its mechanisms. But it was only when chemistry involved too that real progress arrived [1]. It all began in 1973 when a team of physicists and a chemist of XEROX worked on finding out why the copy technology of KODAK competitor was of higher quality. More progress followed twenty years after the Kodak company improved the charging of toners used in printing. Many researchers from IBM, Xerox Corporation and Harvard University contributed to this effort [1].

Since then it has been clear that triboelectricity is a complex phenomenon, whose questions demand the contribution of several scientific disciplines [1].

Μεταπτυχιακή Διπλωματική Εργασία, Αριστείδης Ρεπούλιας, ΑΜ 0014

1.3. Disadvantages of triboelectricity

Triboelectricity charges materials and this can be sometimes an undesirable problem [6]. When it comes for the discharge moment, the built potentials can cause discomfort on human or sometimes even disasters [1].

In the first case, we have the well-known phenomenon of charging when walking on a carpet in dry weather and discharging with a spark when touching a metal doorknob [1] or the spark caused when someone is getting out of a car after a ride, touching the chassis.

In the second case, we may mention the crash of LZ 129 Hindenburg airship, where the combination of a static spark coming from triboelectric charging during the flight, and a simultaneous hydrogen leak is considered as one of the scenarios for its ignition and blast [1,7].

Another disaster scenario can be met even in space, where an astronaut can be charged due to the surface dry conditions of Moon or Mars, making it dangerous when touching the spacecraft, which would cause a discharge and any possible side effects to its electronic equipment [1]. Similarly, it would be possible for an astronaut to carry lunar dust in a spaceship if it adheres on his spacesuit because of contact charging [8].

In pharmaceutical production, contact charging can occur on the moving particles of pharmaceuticals as they flow and blend in powder form during their processing, thus causing non-uniform blending and non-uniform dosages in the products [9].

1.4. Advantages of triboelectricity

On the other hand, triboelectricity phenomenon can be advantageous as the charging between materials can be a necessary key for many manufacturing processes [6].

Triboelectric charging is used broadly today in the technology of copiers and laser printers [1]. Research is also applied to reduce the length scales for this electrophotographic process thus enabling it for uses in nanoscale patterning [8].

Moreover, it is used by novel devices called Tribo Electric Generators (TEG) to achieve continuous charging by exploiting various forms of the surrounding environment's endless mechanical energy (e.g. vibrations, human motion like running or walking, wind flow, acoustic waves, rotating tires or wheels, flowing water etc) [10,11]. This is the reason for calling it a form of green energy too [9].

It is considered that triboelectricity may have played a key role in the origin of life, as it has been found that amino acids can be synthesized during volcanic eruptions from an electrical discharge of ash particles in an appropriate gas mixture, similar to electrical discharges [8].

An important detail concerning the ability to use triboelectric systems with human bodies (through clothing), it is that the produced electricity is not hazardous. No matter if the voltages may be high, the current outputs are very low, while proper management of the power can make a TEG safer to be close to a human body [12].

1.5. Current approach of triboelectricity

Mobile phones, smartphones and various wearable devices are used widely in everyday life across the globe. Sensors are also increasingly attached on many portable or wearable devices to monitor health, quality of training, safety or support systems. Low weight, miniaturization of electronic parts and portability some of the main necessities for today's electronic devices, but their energy sustainability is one of the major ones [4].

Batteries are the most used power sources of the above devices, although they have certain drawbacks like their limited lifetime, their need for frequent replacement and the environmental pollution they cause [11,13]. Moreover, they are bulky [14], stiff and not lightweight [15]. But thanks to the reduction of power consumption of wearable devices [16], a big effort is applied over the last decade to self-power them or replace them using triboelectricity [3].

Another research approach of using triboelectricity beyond the one of power generation to face the global energy demands are the applications in biomedical monitoring, environmental monitoring, chemical sensing and human-machine interfacing [9,10].

1.6. Triboelectricity and textile materials

It is clear that to let triboelectricity build electrical charges, continuous mechanical motion is needed. A way to achieve this continuously and effectively is to exploit human's daily movements. So keeping in mind that textile clothing can be a constant source of friction on a moving human, the integration of triboelectricity into textiles to produce electrical energy becomes more promising.

Another point we shall mention is that thanks to the unique mechanical properties of textile fabrics (e.g. elasticity, flexibility, conductivity, breathability, washability etc) triboelectric generators (TEGs) can inherit them and get improved. For example, to overcome the discomfort or possible inflammations caused by wearable devices made of airtight materials (e.g. polymer films), breathable and skin-friendly textile materials are used instead [15].

The fibrous nature of textiles offers high surface roughness, thus enhancing the effectiveness of the triboelectricity phenomenon and the resultant electrical outputs [17]. Keeping in mind that in textiles a large contact area is available too, their use for energy harvesting becomes challenging [18].

Additionally, considering that textile fabrics can have unlimited structural patterns based on woven, knitted, embroidered or nonwoven technologies, they can also offer unlimited choices for the form of the TEG's contact surfaces. The possibility of choosing from a large number of textile material forms (e.g. multilayered yarns, coated yarns, conductive yarns, nanofibres etc) can contribute to building more complicate TEGs [15,19]. Moreover, the possibility of manufacturing single layer, double layer or even 3D fabrics for TEGs using existing textile machinery, contributes to the development of TEGs [12].

It is is also important to mention that even commonly used textile materials such as cotton, polyester, nylon, etc can all be used in textile TEGS. After applying some appropriate coating of conductive materials (e.g. metal or carbon nanomaterials), these textile fibers, yarns, and fabrics can become highly conductive and used as the TEG's electrodes [19].

Tailorability is a textile property which offers more potentials to TEGs when they are textile-based. It has been shown that textile TENGs can be tailored to cover the demands of the garment designs without malfunctions. Yu et al. presented the case where a textile TENG was cut by scissors into two half pieces, thus each part maintained almost half of the original electrical output. Afterwards, one of the two cut pieces was sewn with another piece of the same dimensions, the same material and same structure. The result was to regain the initial electrical outputs is almost fully [20].

Finally, nanofibres can integrate with textiles and used to build TEGs by forming appropriate membranes. Depending on the structure, a nanofiber membrane may have low weight, small size, adequate air permittivity and a rough nanostructure surface which provides a larger effective contact area than if it was flat, thus providing higher charging efficiency of the TEG. The combination of a nanofiber membrane with an appropriate textile substrate may provide e.g. extra elasticity, extra reinforcement etc. It is important to mention that sensors fabricated with nanofiber membranes achieve higher sensitivity than textile-based sensors [15,21].

2. About Triboelectricity

There are three major questions which must be answered to perfectly explain triboelectricity according to Williams [1]: "Are the charge exchange species electrons or ions, what is the driving force for charge exchange and what limits the charge exchange?"

The target of using triboelectricity is to create a potential difference between the materials by contacting or rubbing one against the other.

The basic principles and mechanisms of triboelectricity have been studied through the potentials created by the contact of different or identical materials, and especially through energy harvesting devices known as triboelectric nanogenerators (TENGs) which are presented later on.

2.1. Triboelectric series theory

Triboelectric series theory is based on a table where materials are classified according to the amount of positive charge that they can transfer (Figure 1). This is usually similar to the electrochemical series table, where materials are arranged according to their tendency to gain or lose electrons [10]. The materials are listed from the top to the bottom of the table, with an increasing tendency to charge negatively (gain electrons).

Μεταπτυχιακή Διπλωματική Εργασία, Αριστείδης Ρεπούλιας, ΑΜ 0014

The direction of charging between the two materials is dependent on the materials involved [1]. Triboelectric series can be used in estimating the direction of charging (positive or negative) for two different materials upon their contact [10].

There have been a few versions of triboelectric series

Positive			Negative
	Polyformaldehyde 1.3–1.4	(continued)	
	Etylecellulose	Polyester (Dacron)Polyisobutylene	
	Polyamide 11Polyamide 6-6	Polyuretane flexiblesponge	
	Melanime formol	Polyethylene Terephthalate	
	Wool, knitted	Polyvinyl butyral	
	Silk, woven	Polychlorobutadiene	
	Aluminium	Natural rubber	
	Paper	Polyacrilonitrile	
	Cotton, woven	Acrylonitrile-vinyl chloride	
	Steel	Polybisphenol carbonate	
	Wood	Polycholoether	
	Hard rubber	Polyvinylidine chloride (Saran)	
	Nickel, copper	Polystyrene	
	Sulfur	Polyethylene	
	Brass, silver	Polypropylene	
	Acetate, rayon	Polyimide (Kapton)	
	Polymethyl methacrylate (Lucite)	Polyvinyl Chloride (PVC)	
	Polyvinyl alcohol	Polydimethylsiloxane (PDMS)	
	(continued)	Polytetrafluoroethylene (Teflon)	

Figure 1. Triboelectric series table of common materials [22].

with small differences in the position of some materials. More specifically, four tables with organic and inorganic materials have been composed by different laboratories in 90 years. Namely, these were published by Coehn in 1898, by Hersh and Montgomery in 1955, by Henniker in 1962 and by Adams in 1987. By comparing these four tables after excluding the inorganic materials, it is becoming clear that the ordering of the polymers is very similar in all the series. Only a few like polyvinyl chloride, wool, silk and polymethyl methacrylate have inconsistent positions [6]. But unfortunately, really poor details are provided about the experimental procedures and conditions used to build these tables. Moreover, these reports don't provide any explanation regarding the positioning of the materials in the table [6].

To achieve greater electrical outputs between the contact of two materials, we must choose a material with a high tendency to offer electrons and a material with a high tendency to attract electrons. This means that the farther the two chosen materials are positioned from each other, the easier they can exchange charges [10]. For example, a pair combining a sheet of Kapton and a sheet of PET will give more voltage than when combining a sheet of Kapton and a sheet of PVC [10].

Another similar table is the semi-quantitative series table by Diaz and Felix-Navarro. This constitutes a better indication of the charging capacity of polymers and came from composing literature reports of polymers contact charging and the four triboelectric series mentioned above. Through this study, it was found that natural polymers (e.g. wool and silk) charge in the range 0.6–1.1pC, while synthetic polymers in the range 0.1–0.5pC. Concerning the polymers with a charge less than 0.1pC, these are questionable to measure because of the inherently low magnitude of the charge in combination with the uncertain past condition of these material samples. The semi-quantitative series table revealed a relation between charging order and the chemical structure of the polymers,

which is as follows: (i) the nitrogen-containing polymers develop the most positive charge (1.2–0.5pC), (ii) the polymers that have oxygen functional groups charge positive (but less than polymers with nitrogen groups), (iii) the halogenated polymers develop the most negative charge (1.6 to 2.8pC) while (iv) the hydrocarbons develop almost no charge.

2.2. Paradoxes of triboelectric series

There are some cases in which the presence of triboelectricity phenomenon is unexpected and unpredictable.

The first paradox is met at the triboelectric series table, in which materials are classified according to the intensity of their tendency to obtain positive or negative charge in relation to others. That means one shouldn't expect the presence of the phenomenon between two surfaces of identical materials [1,5]. But surprisingly, this conventional prediction coming from the old and simplified principle of triboelectric series is in contradiction with what really happens: the phenomenon happens also between materials of identical composition, no matter if pressed or rubbed together, either symmetrically or asymmetrically (asymmetrically occurs when different areas, a small and a bigger, are used) [1,5]. This paradox for the charge transfer occurring from contacting two insulating samples of the same material was stated by Daniel J. Lacks and R. Mohan Sankaran in 2011 [8].

Another paradox concerns the effect of triboelectricity between two insulators, which normally do not conduct electricity neither they charge when they are single. So it is unexplained how and why a charge exchange happens in insulators when using them in pairs although they have no free electrons [1].

As it usually happens, the study of such an unpredictable case can help us to understand better the phenomenon. So, the experimental results of Baytekin et al. as explained in the next paragraph, showed that contact charging can't be attributed or predicted based on the so-called triboelectric series [5].

2.3. The Mosaic surface theory

In the beginning, it was assumed that in a given pair of charging materials one charges uniformly positively and the other negatively. But this assumption couldn't explain why different particles made of the same material, or different regions of the same sample can show different charges than the one initially expected [5]. In 2011, Baytekin et al. used Kelvin Force Microscopy (KFM) which is a high-resolution analysis of the material's surface electrical properties, in order to image the surface potentials over various types of contact-charged surfaces.

It is very important to mention that KFM images do not show the mechanism that occurs during the electrification phenomenon, but only the state of a surface before or after the electrification phenomenon [23]. Similar kind of imaging techniques (Kelvin Probe, KPFM, EFM, force microscopy), can not provide information as well about the

actual course of the contact electrification event, but only for the remaining charges on the surfaces after their separation [23].

The KFM images were a piece of microscopic evidence which revealed that in reality, the charging surface is not homogeneous at all, but it looks more like a random mosaic of positively and negatively charged nanoscopic regions [5]. It was also found that there is significantly more charge per unit area on the electrified surfaces than previously estimated, but the overall charge is relatively small due to the compensation between the positive and the negative regions [5].

Another important founding was that the appearance of charge mosaics is accompanied by changes in surface composition and by the transfer of material between the contacting surfaces [5].

However, the above observations did not explain how and why the charge mosaics emerge. So in order to gain at least some insights into the nature of this process, a series of experiments were performed using Confocal Raman Spectroscopy (CRS) and also X-ray Photoelectron Spectroscopy (XPS). The two relevant observations which were made are that contact electrification is accompanied by the changes in material's composition near the surface and by a lack of homogeneity on the surface just like that of charged mosaics [5].

Interestingly, the KFM scans also revealed that charge does not migrate laterally within the electrified materials, such that the charged regions do not blur and the topological structure of the mosaics is preserved during their discharge. In the absence of lateral charge mobility, discharge is likely due to the collisions of the polymer surface with the molecules, ions, and particles contained in the surrounding atmosphere [5].

So finally it became clear why previous attempts to construct the so-called triboelectric series based on the average material properties often gave ambiguous results. In reality, it is the nanostructure of the material's surface and the fluctuations in this structure that determine the macroscopically observed charging trends [5].

2.4. Charge transfer mechanisms

Evidence has been discovered for both electron and ion transfer under specific experimental conditions, but these data are limited and frequently contradictory. Recent research has demonstrated that charge exchange can also result from the physical transfer of tiny amounts of surface material from one substance to another [1]. The understanding of the phenomenon on a molecular level has begun to emerge only during the last decade.

It has become increasingly clear that more than one mechanism can occur simultaneously, and what happens may depend on the material compositions and conditions of the experiments in ways not yet known [1]. These different contact charging mechanisms are presented below.

2.4.1. Electron transfer.
In the beginning, scientists tried to study triboelectricity phenomenon through physics, as electron transfer could explain the contact charge

between two metals. The key for this to happen is their different work functions [1]. But electrons are not always the medium. Later on, it was found that electrons do not participate in the contact charge of organic polymers [6].

For the case of charging between two metals (when both materials are conductors), it is known that the contact charge exchange results from the transfer of electrons [1].

For the case of charging between a metal & an insulator, there is no general understanding of what carries charges from one surface to the other. Different theories have proposed either electrons or ions [1,2].

For metal-polymer contacts, researchers had found linear relationships between the density of charge created on a polymer and metal work functions, which was presented as evidence for an electron transfer mechanism [1,2]. But considering that there are no free electrons in insulators, this explanation is controversial.

2.4.2. Electric field. The electric field which can be generated by the charges cannot explain the nature of the triboelectric phenomenon exactly, but it can help to understand the fact of reaching a charging limit. According to this theory, the charge buildup is limited when the ambient electric field becomes large enough to exceed the dielectric strength of the surrounding air, pulling apart the electrons from the air molecules and turning it from an insulator to a conductor, thus leaking current away from the material [1].

2.4.3. Ions transfer. The idea for an ion transfer mechanism as a new approach for the explanation of triboelectricity, came twenty years after the Kodak company improved the charging of toners used in printing [1]. Many researchers from IBM, Xerox Corporation and Harvard University contributed to this effort [1]. In this way, the chemistry involved trying to give an answer by accepting that molecules and polymers contain mobile ions which affect the sign and magnitude of the triboelectric charge.

A description of the mechanism is given in a study of the phenomenon by Mahaut [24]. In insulating materials containing mobile ions, a natural layer of water is on the surface and contains mobiles ions. These are transferred during contact with another material's surface [8]. Moreover, ions come from the own surface of insulators, the surfaces have strongly bounded ions that are negatively or positively charged and some less bounded ions of opposite polarity. This creates a disequilibrium when the two surfaces are in contact and the charges are accumulated [25]. For materials that don't have mobile ions, a solution has been proposed; hygroscopic surfaces can absorb water from the air to equilibrium their surface [19]. According to Cornfield, solid dielectrics have naturally their electrical charges produced because of some defects in their crystalline lattice [26]. When these solids are in contact with air, they grab ions of the opposite sign to equilibrate their natural charge. But when friction happens, it destroys this equilibrium so triboelectrification occurs.

2.4.4. Hydroxide ion transfer. The introduction of this theory came in 2008 to explain the charge exchange which can happen on polymers which are non-ionic [1]. According to it, water molecules within the thin water layer between polymers dissociate, with preferential adsorption of the resulting hydroxide (OH–) ions to one surface.

The nature of polymers used is defined by the molecules contained. It is known that many molecules and functional groups are more likely to be donors or acceptors [24]. A table similar to that of triboelectric series was created by scientists to link polymers and charges [6]. Functional groups which have been identified as important factors for triboelectricity [19] are the following (in decreasing donor tendency order): OH, OCOR, C6H5, COOH, CN.

But later in 2011, Baytekin et al. [5] showed that charge can also appear between non-ionic polymers no matter if there is no water layer, so a new theory came up.

2.4.5. Material transfer. This concept was a milestone in the relevant research done so far as it separated from the before established electrons and ions transfer mechanisms, plus it referred to the importance of the contact force too [1].

Using Kelvin Force Microscopy (KFM) Baytekin et al. demonstrated that contact electrification is indeed accompanied by material transfer [5]. This material transfer can be accompanied by charge exchange on a nanoscopic level when two polymers are pressed together for varying times and degrees of pressure and then separated [1]. This kind of charge exchange was unexpected. For centuries, it had been assumed that, in such contact charging, one surface charges to become uniformly positive and the other uniformly negative [1]. Baytekin et al. found that, although each surface develops a net charge of either positive or negative polarity, each surface also supports a random mosaic of oppositely charged regions in nanoscopic dimensions. The net charge on each surface is the arithmetic sum of the positively and negatively charged domains.

Pressing two polymers together, followed by separation, causes small clumps of materials to transfer between the surfaces. After all, it was concluded this material transfer causes bond cleavages which create polymer fragment free radicals, which are very active and react with air's oxygen and water to create charge [1].

Moreover, when rubbing happens, we have an exchange of deeper layer materials and not only the surface's [24]. One can understand that even if the two materials look similar, they don't have the same structure at every layer of material [25].

2.4.6. Material and electron transfer. In 2012, Galembeck et al. took the material transfer mechanism a step further. He sheared, twisted and pressed against each other two films of Teflon and polyethylene. After separation and examination, he found positively and negatively charged domains on them, in agreement to Baytekin's study [1].

Materials extracted from the surfaces with solvents were identified as polymer ions. The Teflon residues were predominantly negatively charged, and the polyethylene residues were primarily positively charged. Galembeck's team proposed this mechanism:

High temperature at the frictional points of contact results in polymer plasticization and/or melting. Shear forces cause breaks in the polymer molecules' chains, forming polymer-fragment free radicals. Electron transfer from the polyethylene radicals to the more electronegative Teflon radicals converts these free radicals to positive and negative polymer ions, respectively, which are known as amphiphiles. Charged macroscopic domains form due to a combination of two factors: Amphiphiles at interfaces are known to sort themselves into arrays when they are in the type of polar environment created by the ions, and Teflon and polyethylene are immiscible [1].

A comparison of the work of Galembeck and Baytekin illustrates the complex interaction between polymer properties and the nature of the contact in affecting the charge exchange mechanism [1].

2.4.7. Other theories. Research advances have also been made for rubbing contacts between two polymers. In 2008, Liu and Bard proposed an electron transfer mechanism on the basis that, after separation, the surfaces were able to induce several electrochemical reactions that can only be caused by electrons [1]. In 2011, Piperno et al. proposed an ion transfer mechanism based on the transfer of material containing polar species [1]. In 2011, also in rubbing contacts between two polymers, bipolar charging patterns were reported by Knorr [1].

2.5. Overall conclusion on mechanisms - A complex relationship
We may also conclude that the electron, ion and material transfer mechanisms may occur simultaneously, depending on the materials and conditions of contact. Especially for the case of contact between two insulators, it is unknown whether the before mentioned material transfer theory is the only or the predominant mechanism [1].

The surprising finding was that contact charging between two polymers relates to their topmost molecular layers, but between a metal and a polymer, it relates to layers beneath the polymer surface. The hypothesis was that the former results from ion transfer between the topmost surfaces and the latter involves electrons tunnelling into the bulk, thus postulating a relationship between charging mechanism and charge penetration depth, which is supported by the fact that ions are known to adsorb to polymer surfaces and electrons are considered to burrow into them [1].

Here arise some questions as for what is the priority of the activation of the above mechanisms. For example, whether the material transfer mechanism is triggered only in the case that friction force is large enough, while the electron or ion transfer mechanism occurs only if friction force is lower. Another question is that if we don't accept the activation of material transfer mechanism in the light contacts, this would support the argument that only pressing and rubbing contacts are highly favourable to the material transfer mechanism. So the lighter contacts would not activate it, thus supporting the original electron/ion exchange hypothesis [2].

In addition to these questions, we can have the affection of additive parameters like the inner morphological composition of the examined polymer's body, so it is becoming understandable how difficult it is to explain the results and the whole phenomenon.

As a result, this complexity has pushed the main interest to focus on building efficient TEG structures, and not to focus on giving an overall explanation of triboelectricity.

2.6. About identical surfaces

There are many problems concerning the triboelectrification of two identical surfaces [24]. It has been considered to be random but some scientists tried to find solutions.

One theory tries to explain this thanks to the asymmetric contact theory. It considers that the two surfaces are not in equilibrium surface states concerning charges of electrons, ions etc. In this case, the disequilibrium induces the triboelectrification charging [25].

Another study also explains the asymmetric contact, considering that at equilibrium the majority of energy states are at their lower state but there are still some at the higher energy state. When the two materials are close to each other, this can drive low energy states and high energy states to be attracted so that the high energy states will reach a lower energy state. This theory is told to be efficient for ions and electrons [8].

Therefore, during triboelectrification between two insulators, it appears that ions transfer happens instantly as the contact is made, but the electrons exchange happens only if the contact between the materials is long enough [27].

2.7. Direction of electrification

A few scientists tried to experiment with some situations described on studies but got results of opposite signs. According to Mahaut [24], this leads to wondering about the direction of triboelectrification. Rose and Yard concluded in their study that the direction of charges was depending on the properties of the dielectric material, not on the metal [26]. A result explains that the loaded force is the major factor to affect the charge flow direction. When the loaded force is large, the charge created is positive and when the loaded force is low, a negative charge is formed when the materials are rubbed. When friction is present, it can change the position of highest occupied levels so change the direction of electrification.

Another solution is to consider that after the charges have built-up, the energy needed to move in the same direction increases so, it becomes more complicated to transfer the charges in the same direction because of the electrical field already created [8]. Finally, a surprising result showed that polymer film as insulators which contain less than 0.1% of water is more suitable to get negative charges, contrary to those which have more than 1% of water.
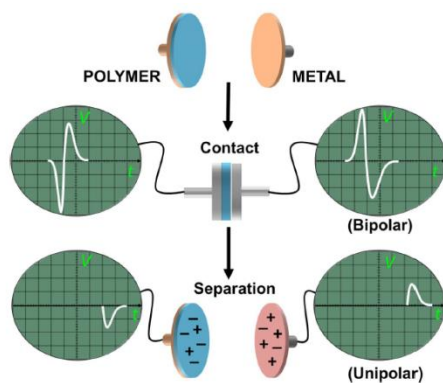
2.8. About bipolar and unipolar signals

When materials are getting close to each other there is an induction phenomenon which represents the largest charge exchange [24]. Musa et al. studied the contact and

separation, by using a tapping device set at different tapping frequencies (1–10 Hz), which allows the contact and separation of two surfaces (a polymer and a metal), for individual detection of the electrical potentials those two stages. The results on an oscilloscope showed that when contact is created, a bipolar signal (both positive and negative) is generated and when the materials separate, only a unipolar (positive or negative) signal is generated (Figure 2). This can be seen in our oscilloscope display, during our experimental part as well (Figure 3).

Researchers assumed that initial charges at the surface of the polymer were of both signs to explain the bipolar signal [24]. The signals of contact and separation can be explained by a bond-breaking that releases free charges. Therefore, as the materials are quickly separated, the charges don't have enough time to equilibrium and the materials are charged either positively or negatively. The polymer keeps electrons at its surface so is negatively charged and the metal keeps its loss of electron so it is positively charged. After leaving the charged surfaces, the polymer slowly equilibrates its charges with air and metal only equilibrates its charges quickly when connected to the ground [23].

Figure 2. Bipolar and unipolar signals [23].
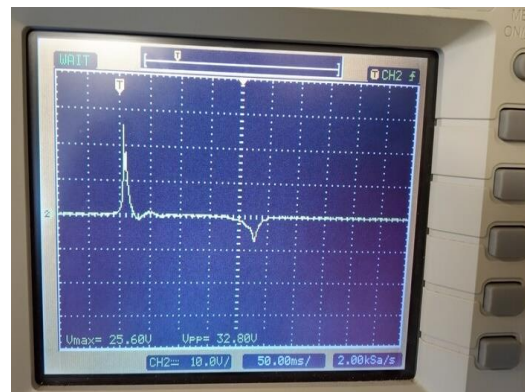
Figure 3. Image of the bipolar and unipolar signals as seen during our experimental part.

3. About Triboelectric Generators (TEGs)

Many efforts have been applied over the last decades to harvest electrical energy based on the triboelectricity effect by building novel structures known as TEGs and TENGs and store e.g. in capacitors to power supply small or low energy consumption electronics.

3.1. Definition

A Tribo Electric Generator (TEGs) is defined as the energy-harvesting mechanism which converts the external mechanical energy into electricity, based on the principles of triboelectricity and electrostatic induction, by using various set-up modes as described below [4,11]. When the nanotechnology is introduced in the building of a TEG then it is called Tribo Electric Nano Generator (TENGs).

3.2. History

It all began in 2006 when Wang et al. demonstrated the first piezoelectric generator [28]. Since then, lots of different structures and materials have been used. In 2012, Prof. Zhong Lin Wang's group at Georgia Institute of Technology demonstrated the first TENG [11]. Into the next 5 years, the research on TENGs increased exponentially [9], becoming very promising for the near future.

The interest for energy harvesting using triboelectricity and nanotechnology has been increasing over the last years, due to the increasing presence of wearable electronics or sensors and their need to become self-powered [10].

3.3. Brief description

The simplest form of TENG consists of two separate materials (films usually) which show different electron affinities on their surfaces based on their position in the triboelectric series table [9]. A pair of electrodes are attached to the materials backsides [11]. When their front sides of the two materials are brought in contact, rubbed or separated, opposite electrostatic charges appear into them thus inducing charges to the electrodes too. As long as the electrodes are connected through an external circuit, a current is transferred through it for further use (e.g. lighting a led) or management (e.g. storage).

The pair of electrodes play a double role [10]. Firstly they produce equal but opposite sign electrical charges thanks to the induction with each of the materials. Secondly, they transfer the produced current to the desired target (e.g. a circuit, a led or a capacitor).

Research has shown that organic materials are more useful to be used [11]. In this case, the TENGs may also be called as organic triboelectric nanogenerator (OTENG).

It is not a rule that a TEG must be used all alone. Two or more TEGs can be connected in parallel with the same or opposite direction [10]. In the first case, the total current is enhanced while in the second case it is reduced. Thus we can increase the total output current and power per unit area by connecting multiple TEGs in parallel and assemble them all together layer by layer thanks to their thinness [10].

The most suitable materials for creating a TEG can be chosen based on a triboelectric table in which all materials are ranked by the magnitude and type of charge that appears on their surface during friction. There are four basic operational modes for the TEGs [3].

3.4. Characteristic measures and necessary instruments

No matter of their structure TENGs can be characterized by the following measures: the open-circuit voltage V_{oc} which is measured using a digital oscilloscope, the short circuit current I_{sc} which is measured using a low noise current preamplifier, the power density (output power per unit area) which is calculated with the formula $P=V \cdot I$, and also the capacitor charging [9].

Moreover, laboratory sized TENGs can give output voltages ranging between few millivolts and hundreds of volts, but their output current is very low ranging between nA and mA. These low currents are difficult to measure without a low noise current

preamplifier which can even measure input currents of the fA or pA range but is pretty expensive. However, lower-cost approaches have been reported to measure the low current of TENGs [9].

3.5. Output values

A simple TEG structure which is contained of two polymer sheets with different triboelectric characteristics, stacked without interlayer binding and covered on their backside with metal films, can produce a voltage of up to 3,3V and a power density of ~10.4mW/cm³ [10] when deformed.

According to Chacko et al. the output power density of TENG has increased for five orders of magnitude within 2016-2017. The power density has attained 313W/m², volume density has attained 490kW/m³, and conversion efficiency of 60% has been demonstrated [11].

Moreover, according to a 2018 research of Molnar et al. the maximum energy density of TEGs has reached 1200W/m² or 490kW/m³ with an efficiency of ~50-85% [3].

When a bridge rectification circuit is added in the circuit a TEG (Figure 4), we can exploit the negative generated charges too, and store it all in connected capacitors [4,10].
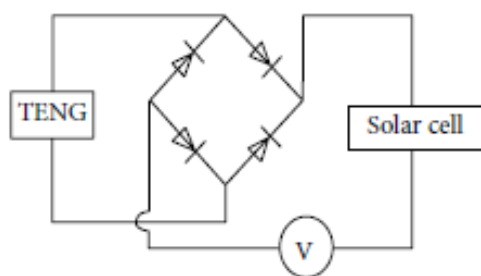
Figure 4. Schematic illustration of the bridge rectification circuit.
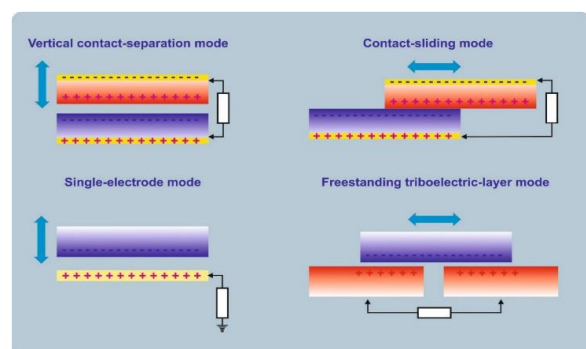
Figure 5. The motion directions of the four modes of triboelectric generators [3].

3.6. Advantages

One of the biggest advantages is the potential of TEGs to harvest all the forms of endless mechanical energy of the surrounding environment instead of losing it, like the ones coming from human activities (e.g. arms motion, walking or running), car's rotating wheels, wind flow, sea waves, flowing water, sound vibrations etc [10,11]. Thus it is considered to be a new coming form of green energy [9] beyond the more popular solar and wind energy [9] which have attracted more attention [29].

Another advantage of TEGs is their possibility of fixing them into moving mechanical objects (e.g. clothing) or systems (e.g. a rotating tire) thanks to their small size and lightweight [3].

The possibility of applying the 3D printing technology on TEGs is another advantage characteristic they have. Thus more complicated and efficient TEG structures can be built [3].

Concerning their fabrication cost, we must concern that simple two-sheet TEGs like the one developed by Wang et al. [10] in the laboratory environment, may not demand the use of expensive materials and equipment, thus offering the advantage of low-cost commercial production.

To sum up, depending on the materials and the structure used for TEGs they can be simple, reliable, low cost in manufacturing and efficient [9,11]. But we shall also mention the low fabrication cost is not a rule. To improve the electrical outputs of TEGs, more expensive complex structures using more expensive efficient materials may be required, thus increasing their industrial production's cost.

3.7. The 4 modes

In total, there are four fundamental operational modes which can be used in TENGs: vertical contact-separation mode, in-plane sliding mode, single-electrode mode and free-standing triboelectric-layer mode [4,9]. These have different motion directions of the contacting involved (Figure 5). However, sometimes, the fourth mode is omitted [11]. The way each mode works is explained and demonstrated below.

3.7.1. Vertical contact-separation mode. As an example, let us consider the simplest construction of TENG (Figure 6). Two different dielectric films face each other, on the upper and lower surfaces of which electrodes are located. The physical contact of two dielectric films leads to the accumulation of an opposite charge on their surface. When the external force separates these two surfaces from each other (leads to an increase in the gap between them) a potential drop is created. If two electrodes are electrically connected to the load, the free electrons from one electrode will flow to the other electrode to create an opposite potential that balances the electrostatic field on the electrodes [3,30].

3.7.2. In-plane sliding mode. Let us consider a generator of similar structure, suitable for the mode of separation of contacts. When two dielectric films are in contact, the parallel sliding of two surfaces also creates triboelectric charges on both surfaces (Figure 7). In this case, the transverse polarization arises along the sliding direction, which leads to the flow of electrons to the upper and lower electrodes, and they completely compensate for the field created by the triboelectric charges. Periodic expansion and convergence of the two plates generate an alternating current at the output. This is a sliding mode of TENG. The slip can be a movement in a plane, a cylindrical rotation or a rotation of a disk [3,31].

3.7.3. Single-electrode mode. In some cases, the objects that are part of TENG cannot be electrically connected to the load, since they are mobile, such as a person walking on the ground. In order to generate the energy in such a case, TENG with a single electrode was created (Figure 8). This variant corresponds to an equivalent circuit in which the

electrode on the bottom of the TENG is grounded. If the size of TENG is finite, then the approximation or removal of the upper and lower objects will change the local distribution of the electric field, under which the electrons between the lower electrode and the ground exchange are exchanging [3,32].
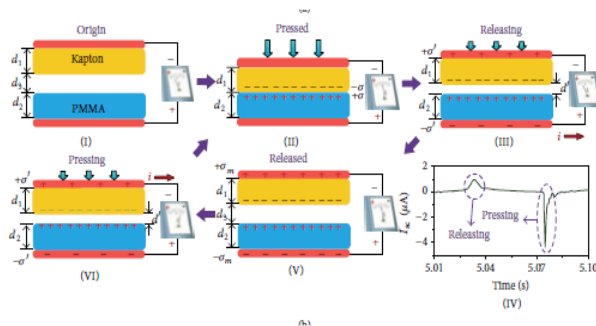
Figure 6. Vertical contact-separation mode mechanism [4]
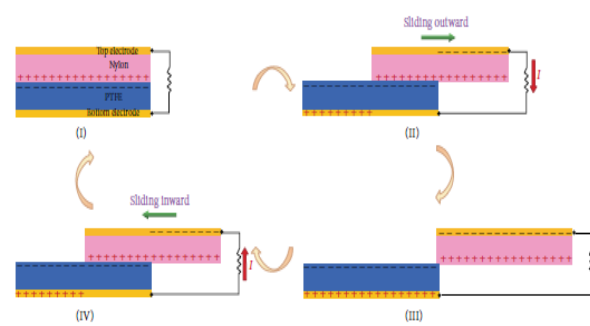
Figure 7. In-plane sliding mode mechanism [4]
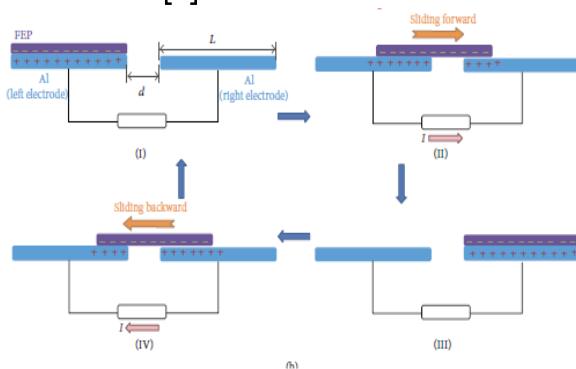
Figure 8. Single-electrode mode mechanism [4]
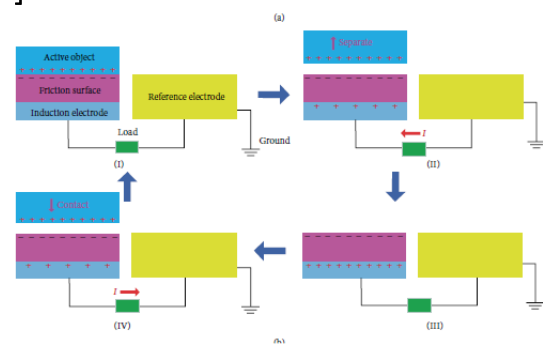
Figure 9. Free-standing triboelectric-layer mechanism [4]

3.7.4. Free-standing triboelectric-layer mode. In nature, moving objects are naturally charged due to contact with air or other objects (for example, shoes on the floor). As a rule, the charges remain on the surface for several hours (Figure 9). If we take two identical electrodes coated with a dielectric layer, the size of the electrodes, and the distance between them, will be the same as the size of the object moving above them, the approach or removal of the object to one or the other electrode will lead to an asymmetric charge distribution in the surrounding, compensating by this the local distribution of the potential [3,33].

3.8. Comparison between modes
We shall mention that the contact-separation mode converts the mechanical energy of a periodic contact-separation oscillation of the tribo-pair materials into electrical energy, with high efficiency, and has wider applications in sensoring or energy harvesting. The sliding mode depends largely on the contacted area of the tribo-pair materials and is

applied in diverse forms of mechanical motions. The single-electrode and the freestanding triboelectric-layer modes harvest energy from arbitrary moving objects [34].

Experiments were made to achieve a comparison between a vertical contact-separation and an in-plane sliding mode TEG and showed that the characteristics of their electrical outputs are very different (Figure 10). The current generated by a TENG based on the in-plane sliding mode has a smaller peak value (~15μA) but a longer pulse, in comparison to that generated by a TEG based on the contact-separation mode, which has larger peak value (~240μA) but a shorter pulse. This happens because of their different charge separation process: in the in-plane sliding mode, the length of the effective displacement is large (equal to the dimension of the plate along the sliding direction), so that the charge transfer takes much longer time, while in the vertical contact-separation mode, the length of the effective displacement is small (less than 1 mm) so that the charge flows faster [31].

An important detail that has to been taken into account when designing a contact-separation mode TEG, is that in order to realize the vertical charge separation, an air gap is mandatory to be created at the separation step, which usually requires sophisticated design of the TEG's structure (e.g with springs) and might make difficult their practical applying sometimes [31]. On the other hand, a gap is not necessary for example between the contacting surfaces for in-plane sliding mode TEGs, thus making them more advantageous.

3.9. Simple TENG structure examples

Based on the four before mentioned operational modes, scientists have combined materials and electrodes to harvest energy from mechanical motion through simple TEG structures. A few such examples are presented below.

Figure 10. Comparison of the generated current during a cycle, between in-plane sliding mode and a vertical contact-separation mode.

3.9.1. Example 1.

A low-cost robust TENG (Figure 11) was built using PET/ITO and Kapton by Mallineni et al., and reached 480V and 1.7mW, for a contact force of 50N/cm² and a 2Hz frequency. The TENG's constant performance lasted for more than 20,000 cycles [35].

3.9.2. Example 2.

Wang et al. demonstrated a TENG based on the in-plane sliding mode (Figure 12) using a pair of materials a polyamide 6.6 (Nylon) film and a polytetrafluoroethylene (PTFE) film. When using a linear motor to move the guided plate on to another two plates, with a constant acceleration-deceleration rate of ±20m/s², the coming voltage reached ~1300V, with a current density of 4.1mA/m², and a peak power density of 5.3W/m² [31].

Figure 11. Schematic of a simple vertical contact-separation mode TEG built by Mallineni et al. [35].

Figure 12. Schematic of a simple in-plane sliding mode TEG built by Wang et al [31].

3.10. Textile based TENG structure examples

As it was mentioned in the first section, thanks to their mechanical properties, textile materials (multilayered yarns, coated yarns, conductive yarns, nanofibres etc) can integrate into flexible and breathable TEGs to harvest triboelectricity from daily human motion, wind flow etc [15]. Moreover, they are characterized by advantageous lightweight, flexibility and portability making them wearables [36]. A few examples are presented below.

3.10.1. *Example 1.* In 2014, Zhong et al. developed the first fiber-made TENG [14]. By twisting a carbon nanotube coated cotton yarn and a carbon nanotube coated cotton yarn with an extra coat of polytetrafluoroethylene (PTFE), was built a twisted double yarn which can operate as TEG (Figure 13). Many of these were afterwards sewn into a woven fabric, thus offering an average output power density of ~0.1 μW/cm² when stretching This work established the first proof-of-concept that the TEGs can be woven into fabrics and exploit human's motions.

3.10.2. *Example 2.* TENGs have been implemented in textiles at a nano-level too [12]. For example, Win et al. developed a breathable, stretchable TENG using nanofiber membranes [37]. Initially, polyvinylidene fluoride (PVDF) and thermoplastic polyurethanes (TPU) nanofibers are produced through electrospinning (Figure 14). Afterwards, they are processed to build a thin irregular pile on the surface of elastic conductive textiles, thus forming a nanofiber membrane on them. Thanks to the rough surface of these membranes, high friction is achieved, while the elasticity of the textile underneath structures provides sufficient stretchability to rub and contact the membranes.

3.10.3. *Example 3.* Zhou et al. built a woven TEG (Figure 15) by cutting stripes out of a polyester and a nylon sheet, attaching additional silver electrodes stripes on them and weaving them into a woven fabric [15,38].

3.10.4. Example 4. Another example based on a different textile structural form is the TEG built by Li et al. [15,39]. In this case, a commercial yarn-winding machine was used to make compound yarns (Figure 16). These had a silver core and a nylon (PA6) shell, or a silver core and a polytetrafluoroethylene (PTFE) shell. By weaving these yarns separately, two different fabrics were built. By attaching them together a TEG was built. It was placed on a cloth, letting the two fabrics to come in contact and rubbed against each during human motion. Flexibility and washability were achieved, while a capacitor could be easily charged from 0 to 5V within 100s for a given TEG size of 4cm x 4cm.
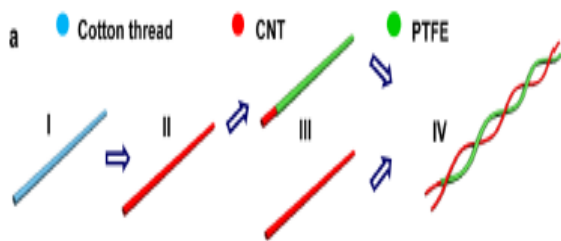
Figure 13. Schematic diagram illustrating the building principle of the textile TENG.
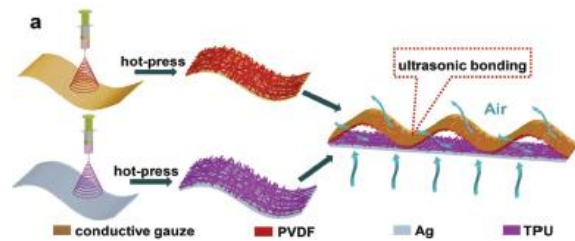
Figure 14. Illustration of the building principle applied by Win et al [37].
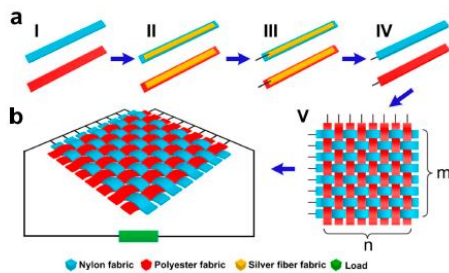
Figure 15. Fabrication process and structure of a woven TEG by Zhou et al.
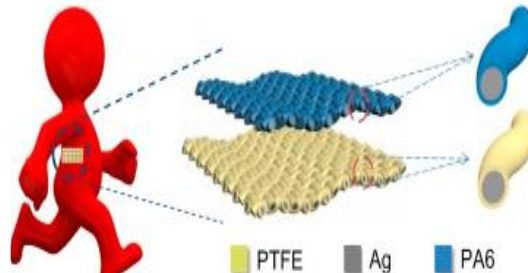
Figure 16. Woven wearable TEG made of core-shell yarns.

3.10.5. Example 5. Dudem et al. using polyaniline (PANI) coated cotton fabric, built two TEGs, one based on the vertical contact-separation mode and another based on the single-electrode mode. The first reached ˜350V, ˜45μA and 11.25W/m² (for compression force of 5N), while the second ˜120V and 4.2μA.

3.11. Advanced TENG structure examples
In order to achieve optimized efficiency in TEGs and meet the large needs of energy, more complicated designs than the regular of two sheets have been implemented in laboratories. Easy fabrication and low cost are always prerequisites.

Moreover, special materials in special forms may be used to increase efficiency. For instance, keeping in mind that nanofibres are easily triggered by small physical motions

Μεταπτυχιακή Διπλωματική Εργασία, Αριστείδης Ρεπούλιας, ΑΜ 0014

and that ZnO is a highly tensile material, resistant to deformations and widely used in nano-coating, Chacko et al. developed a TENG using ZnO coated nanofibres [11].

To understand the limitless combinations of materials and designs applied on advanced TEGs, a few examples are presented below.

3.11.1. Example 1. The first example of TENG is the one developed by Molnar et al., using three layers (Kapton, PTFE, Aluminium foil) which are bent into a zigzag structure, thus giving it the shape of an accordion as seen in [3]. This combination equals to a TENG with five layers connected in parallel (Figure 17). It has the advantages of being light (7g), easily manufactured and flexible to bend, easy to integrate into clothes and with a virtually unlimited term of operation offering relatively high energy power. This TENG has dimensions of 3.8 x 3.8 x 0.95cm and can give 0.65mA and 215V. Moreover, it provides a surface energy of 9.76mW/cm^2 and a bulk energy density of 10.24mW/cm^3 for an applied force of 400N.

3.11.2. Example 2. Another case for large scale energy harvesting consists of two PMMA substrates that are connected by four springs to maintain a gap and an electrode appropriately attached (Figure 18) [4]. The contact electrode is a gold thin film with uniformly sized and distributed nanoparticles (which further increase the effective contact area, thus enhancing the electrical output of TENGs), play two roles, that of electrode and contact surface too. On the top side, another film of gold is employed as another electrode, sandwiched by a layer of polydimethylsiloxane (PDMS) and the substrate. A mechanical shaker is used to apply impulse impact. For a contact force of 10N, the voltage was between zero and a plateau value and current (exhibiting an AC behaviour) was between 160–175μA, while for 500N, the current reached 1.2mA (because the full contact area of the two materials can be achieved by a larger force). Using resistors as external loads, for 500N, the power output reached 0.42W.

3.11.3. Example 3. Furthermore, a three-dimensional TENG based on an in-plane sliding mode has been demonstrated for large scale energy harvesting [4]. It has layer-by-layer stacked polyvinyl chloride (PVC) and aluminium as friction materials as seen in Figure 19. The efficient fiction area is largely increased owing to the multilayered structure. The voltage reached was 800V with a current of 120μA. The results show that the output power is maximized at around 27mW at an external resistance of about 8MΩ. In this case, the 3D TENG can drive the microelectronics or other sensors. Moreover, after a run of over 1000 cycles, it showed significant stability as for the current output produced.

3.11.4. Example 4. Keeping in mind that synchronizing the outputs of all multiple units in a TEG can potentially enhance the output current, an innovative design of TENG integrating rhombic gridding was developed (Figure 20). It is considered as a low cost and robust approach because of the multiple unit cells connected in parallel. PET was used as a substrate, while in each unit cell, an aluminium thin film with nanopores served

not only as a triboelectric surface but also as an electrode. PTFE coated copper was employed as another contact surface. It was shown that the accumulative induced charges increased dramatically [4].
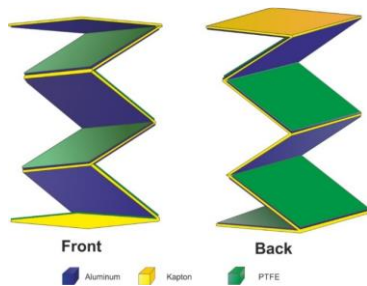
Figure 17. Advanced TENG example 1.
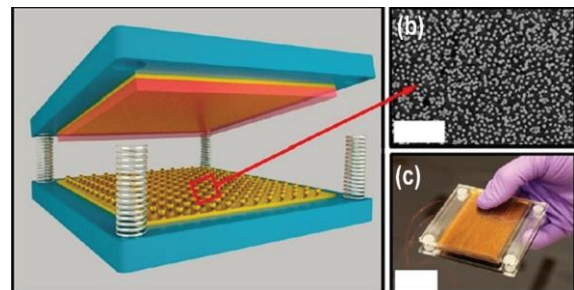
Figure 18. Advanced TENG example 2.
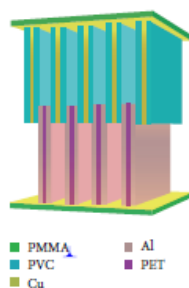
Figure 19. Advanced TENG example 3.

Figure 20. Advanced TENG example 4.
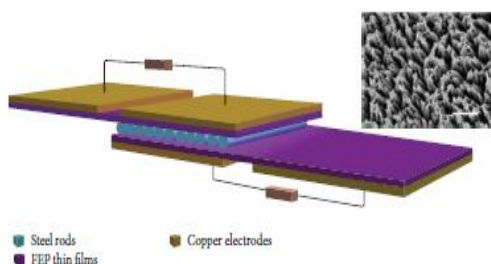
Figure 21. Advanced TENG example 5.
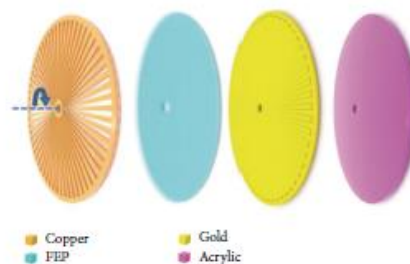
Figure 22. Advanced TENG example 6.

3.11.5. Example 5. Another advanced example of TENG is a multilayered structure which generates periodically changing triboelectric potential and alternating currents between electrodes [4]. It consists of a group of rolling steel rods sandwiched by two layers of FEP thin films and copper which are coated onto the FEP film as back electrodes, as seen in Figure 21. As the top FEP-layer moves from the left end to the right end of the bottom FEP-layer, the steel rods also move from the left part to the right part of the bottom layer-FEP. This way triboelectric charges are introduced on both surfaces of the FEP thin films. Increasing the velocity of movement from 0.1 to 0.5m/s, the maximum output power increases too.

3.11.6. Example 6. Based on multilayered materials, Zhu et al. demonstrated a planar structured TENG with two radial-arrayed fine electrodes, which is composed of mainly two parts: a rotator and a stator, as shown in Figure 22 [4]. The working principle of the TENG is based on the free-standing triboelectric-layer mode, generating alternating currents between electrodes. When the TENG works at a rotating rate of 500rpm, current can reach 0.5mA. and the peak-to-peak voltage can reach 870V. It was found that the output power is proportional to the rotation rate. For a rotating rate of 3000rpm, an average output power of 1.5W was obtained.

3.12. Hybrid TENG structures for optimized efficiency

Going a step further than advanced TEGs, many attempts have been devoted to combining different electrical harvesting devices, thus developing hybrid TEGs. A few examples are presented below.

3.12.1. Example 1- Hybridized Electromagnetic-Triboelectric Nanogenerator. Hu et al. developed a hybrid generator composed of a TENG and an electromagnetic generator (EMG) [4]. When there is a mechanical disturbance, the TENG operate in the vertical contact-separation mode and in-plane sliding mode as shown in Figure 23. Likewise, the magnetic flux in the coil will change, and an electric output will be generated in the coil because of electromagnetic induction. It was indicated that the hybridized nanogenerator has a much better-charging performance than that of the individual energy harvesting units. We might also mention that the TENG gives high voltage and low current outputs, with large output impedance, while the EMG gives high current but low voltage outputs, with a small output impedance. Thus, transformers are applied to the measurement system.

3.12.2. Example 2 - Hybridized Triboelectric Nanogenerator integrated with Solar Cell. Another hybrid generator combining mechanical and solar energies has been developed too [4]. This is based on the hybridization of the TENG with Si solar cell, where a PDMS layer plays a dual role of the effective triboelectric-layer for the TENG and the high transparent protection layer for the Si solar cell (Figure 24). The rectified TENG and the solar cell are connected in series. The Si solar cell's output voltage reaches 0.6V and current 18mA. After attaching a bridge rectification circuit, the TENG's output voltage reaches 2.5V, and the peak output voltage of the hybrid nanogenerator can be enhanced owing to the TENG and reach 12V.

3.12.3. Example 3 - Hybridized Triboelectric – Piezoelectric Nanogenerator. Jung et al. developed a hybrid TEG which integrates the principles of piezoelectric (PNG) and triboelectric (TEG) generators. This hybrid generator carries the advantages of combining a high piezoelectric output current (12mA/cm^2) and a high triboelectric output voltage (370V). The average power density was 4.44mW/cm^2 *[40]*.
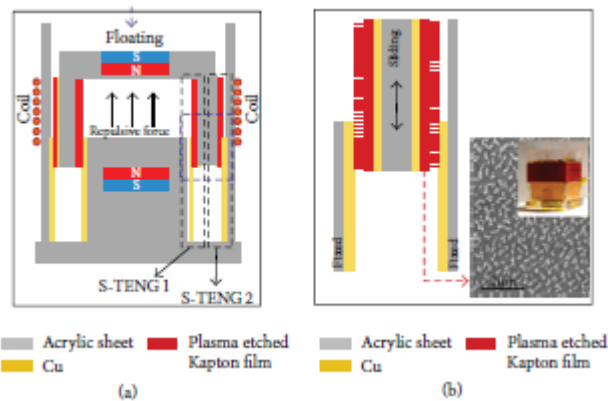
Figure 23. Hybrid TENG example 1.
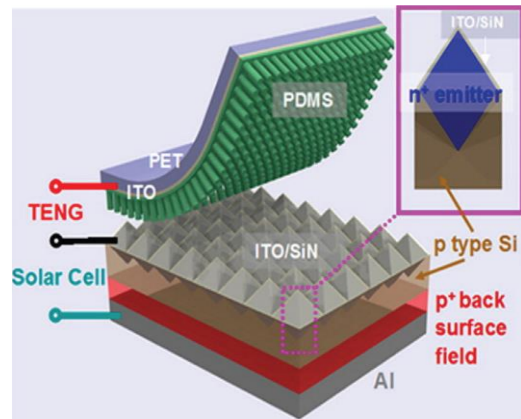
Figure 24. Hybrid TENG example 2.

3.13. Parameters affecting the electrical output of TEGs

As it has already been mentioned, the parameters which predominantly influence the electrical output of TEGs, are the materials involved [9,10] and the structural design [3]. But these are not the only ones affecting the intensity of the electrical outputs [3]. Attention must be paid to numerous external parameters in order to control correctly the measuring procedure (e.g. surface's area, applied force during contact, friction intensity, environmental conditions, way and speed of surface separation etc). This way appropriate reliability and repeatability will be achieved.

This is getting very crucial especially in the delicate case of comparing the electrical outputs of different TEGs setups. If a human is involved in the measuring procedure, then repeatability is low and the comparison would be ambiguous. Thus the use of an automated device where material samples can be inserted and then tested under constant conditions is recommended. Such an example is the attempt by Fan et al. who used a linear motor in a cyclic agitation (at 0.33Hz and 0.13% strain) to periodically bend and realise a sandwiched structure TEG and measure its electrical outputs [10].

The main parameters which influence the output voltage and current, are presented below:

3.13.1. Materials choice. The combination of materials affects the electrical outputs of a TEG [9,10]. The longer the distance between the positions of the selected materials in the triboelectric series table, the more intensive will be the phenomenon [10]. For example, a TEG combining sheets of Kapton and PET will give more voltage than when combining sheets of Kapton and PVC [10].

3.13.2. Duration of contact. In experiments carried out by Baytekin et al., the method of Kelvin Force Microscopy (KFM) was used to verify that the phenomenon seems to be independent of the surfaces contact times when these were between 2s and 1.5h [5].

Μεταπτυχιακή Διπλωματική Εργασία, Αριστείδης Ρεπούλιας, ΑΜ 0014

3.13.3. Speed of contact and separation. In the experiments carried out by Baytekin et al. using Kelvin Force Microscopy (KFM) to demonstrate new findings on the contact electrification charging (equal to contact-separation TEG mode), it was verified that the results did not depend significantly on the speed through which the surfaces were separated [5].
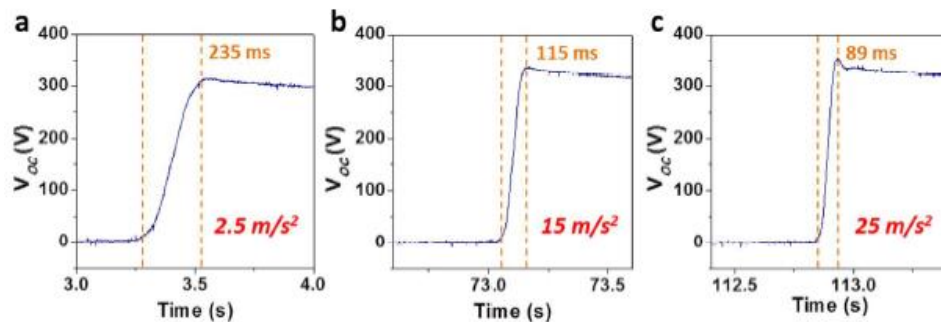
Figure 25. The form of the voltage rising for three different sliding accelerations.

Moreover, Wang et al., after developing an in-plane sliding TENG, he showed that the faster the sliding speed is, the faster the voltage changes (increases or decreases) [31]. This is reasonable as at a higher acceleration/velocity of separation, the elapsed time for travelling a fixed displacement will be shorter, which means a shorter time for the voltage to jump up to the plateau as seen in Figure 25. On the other hand, the voltage doesn't have a significant increase when increasing acceleration, which is also consistent with the theoretical expectation that voltage is only determined by the displacement (for the case of in-plane sliding TENGs).

3.13.4. Frequency of compression or rubbing. The frequency of bringing in contact, rubbing or separating the two material sheets of a TEG, can affect its electrical output depending on its structure [9].

For example, in the case of a bending TEG structure with two polymer sheets designed by Fan et al. [10], it has been shown that frequencies of the range 0.33-1Hz did not affect significantly the current output, while frequencies higher than 1Hz increased it. This possibly happens due to the lack of time for the two sheets to discharge completely before a new charging circle, thus causing an accumulation of residual charges on the electrodes [10].

In another case of bending TEG structure with two polymer sheets [21], it has been shown that when increasing the frequency of the applied pressure from 1 to 5Hz the voltage output increased too (due to external electrons flowing to reach equilibrium in a shorter time), while for the range of 5-7Hz the voltage was constant, and for 10Hz it decreased (due to the under-releasing of the sandwich-shape nanogenerator, which means that the TENG cannot recover to the original state due to the long recovery time).

3.13.5. Compression force on contacting surfaces. In the experiments carried out by Baytekin et al. using Kelvin Force Microscopy (KFM) to demonstrate new findings on the contact electrification charging (equal to contact-separation TEG mode), it was verified that the results did not depend significantly on the pressure applied during contact (ranging from 0.01 to 4.5MPa) [5].

But in another case where bending and releasing is applied, the applied force on the TEG sheets affected its outputs. In the case of a bending TEG structure with two polymer sheets developed by Fan et al. (based on contact-separation mode), it was found that increasing the applied strain while bending and releasing the TEG, resulted in increasing of the electrical output current due to better contact between the surfaces [10].

In another research, increasing the compression force on a contact-separation mode TEG (built by Dudem et al.) increased also the electrical outputs [17]. More specifically, the maximums were obtained at 10N, but the values remained almost constant even after increasing the compression force up to 30N [17].

We must also mention the crucial importance of applied pressure for in-plane sliding mode TEGs. If the two plates during the overlapping phase are not kept in fully tight contact, then little electrical outputs are generated. So to get the best performance of an in-plane sliding mode TEG, then it is mandatory to keep an intimate contact between the two plates at the overlapping area during all the sliding phase [31].

In the case of TENGs with curved surfaces, experiments carried out by Xu et al. showed that increasing the applied force between the two curved surfaces is likely to lead to a reversal of charge transfer direction between them [41].

Moreover, it has been found that the tension of a surface to charge positively or negatively, may be affected and even reversed by the applied contact force [8]. Sun et al. carried out some experiments by contacting or rubbing AFM tips against a SiOx surface under various forces and measuring the generated electrostatic charges of the surface immediately with Kelvin Force Microscopy (KFM). A charge sign reversal phenomenon occurred in both friction and contact experiments. It was observed that when applying a large force (larger than 550nN in this experiment) then a positive charge formed on the surface. When applying a small force then a negative charge formed [42].

3.13.6. Structural design of TEG. Depending on the simple (e.g. two material sheets) or more advanced (e.g. multiple layers and sheets) structure used, TEGs provide different electrical outputs [3,4,10]. An example is the TENG developed by Molnar et al., using three layers (Kapton, PTFE, Aluminium foil) which are bent into a zigzag structure, thus giving it the shape of an accordion [3]. This combination equals to a TENG with five layers connected in parallel giving higher electrical outputs than more simple structures.

3.13.7. Roughness of contacting surfaces. The roughness of the contacting surfaces affects TEGs electrical outputs [3]. By increasing it, the effective area of friction gets larger [21].

For example, in the case of polymers, the higher the roughness, the easier happens material transfer between the TEG's surfaces, thus expecting higher electrical outputs.

Building microstructures or nanostructures with sufficiently rough surfaces have been effective. An example is a TEG whose surfaces were composed of nano-scale holes in the shape of inverted pyramids (created with the replication process with mold) [21]. This TEG provided 100% more voltage than when using flat surfaces.

In order to enhance a TEG's performance, the functionalization of its TEG's surfaces with plasma is often used. Yeong Kim et al. examined particularly the effect of Ar plasma treatment on a polytetrafluoroethylene (PTFE) based TEG, and found a consequent increase in the roughness and number of polar oxygen ions on the PTFE surface (thus increased hydrophilicity). After a 10min Ar plasma treatment, the PTFE based TEG generates a 715V V_{OC} and a 16μA I_{CC}, which are almost 79 and 32 times larger than those for as-received PTFE [43].

However, we must mention that it is not known what increases charge transfer when rubbing two materials, where the two possible explanations could be either the increase of their contact area thanks to their roughness either the stress imparted from rubbing [8].

3.13.8. Area of contacting surfaces. It is expected that wider surfaces provide more available space to participate in bigger charge transfers, thus higher electrical outputs. Logothetis et al. measured the generated voltage on samples of different surface areas and showed that increasing the contact area increases the voltage outputs too [18].

Yu et al. presented the case where a textile TENG fabric was cut by scissors into two half pieces, thus reducing to more than half the original electrical outputs, while when two half pieces were sewn they regained the initial electrical outputs almost fully [20].

In the case of textile TEGs, it has been demonstrated that fabric's patterns, being related to the contact area, can affect seriously the TEG's performance. Kwak et al. calculated the contact area of three knitted fabrics which had different knitting patterns (plain, double, rib). Then he measured their output voltages depending on their morphology and the stretching applied. It was found that double and rib patterns showed superior stretchability, especially the second, thus boosting the generated output voltages of the TEG. [44].

In the case of an in-plane sliding mode, Wang et al. showed that when the displacement of the upper plate over the lower plate increases (thus their contact area decreases) the voltage output increases [31]. It was also found that the measured transferred charge density displays a linear relationship with this displacement.

The effect of contacting surfaces areas is found also in the direction of charging when rubbing asymmetric contacts of identical material. Rham et al. observed that the average charge transfer direction is found to be material dependent. For example, when contacting two asymmetric Teflon surfaces, the larger area region charges positively,

while when contacting two asymmetric Nylon surfaces the larger area region charges negatively [45].

3.13.9. Thickness of contacting surfaces. Until the moment of writing this review, no exact information has been found on whether the higher thickness of a contact surface can influence positively or negatively the electrical output of a TEG. However, in almost all cases, it is reported that materials in the form of thin films are used.

3.13.10. Density of contacting surfaces. In the case of textile TENGs, fabric textures (e.g. stitch density as for knitting) can make a major difference to their output performance. Experiments carried out by Huang et al. showed that the face side of some knitted fabrics gave twice the voltage of the backside. This happens because the available contact area is higher at the front side where loops are exposed, while it is lower at the back side where loops are entering fabric's body [46].

Laminated surfaces offer the advantage of microstructural roughness, thus of higher performance of the textile TEGs. Huang et al. fabricated laminated fabrics under specific pressures and compared their performances on TEGs. It was found that increasing the applied pressure during the fabrication, increased the TEG's performance too, until some certain high pressure, where the performance decreased, more probably because of the destruction of the ideally formed TEG's surfaces [46].

3.13.11. Curvature of contacting surfaces. Xu et al. applied experiments to compare various combinations of differently curved contacting surfaces of a TENG, made of identical material and sizes (Figure 27). Results showed that when the two surfaces were flat there was no certain tendency of charging direction. On the other hand, if the contacting surfaces had a curvature, then convex surfaces show a tendency to get negative charge and the concave ones a tendency to get positive charge [41].

It is worth mentioning that theoretically, if the two surfaces of identical material and size of the TENG were perfectly flat in a nano-micro scale, then there would be no curvature differences, thus no different surface energies and no electron transfers, thus no charge [41].

3.13.12. Ambient temperature. It has been mentioned that ambient temperature and relative humidity can affect the electrical outputs [3,9]. Mallineni et al. examined the effect of temperature on a simple TENG which he had developed, using PET/ITO and Kapton electrodes [35]. The TENG's voltage output did not show any deterioration until 60°C, being ~480V. For temperatures above 60°C, it decreased gradually to ~240V. For temperatures above ~110°C a plastic deformation of the PET electrode occurred so the test was stopped (Figure 26).
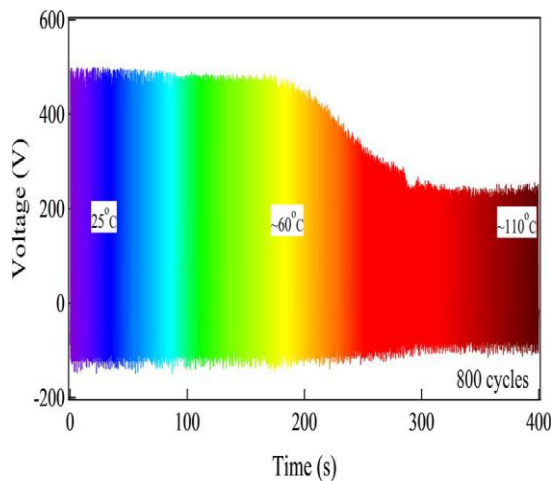
Figure 26. Performance of the TENG by Mallineni et al. as a function of temperature.
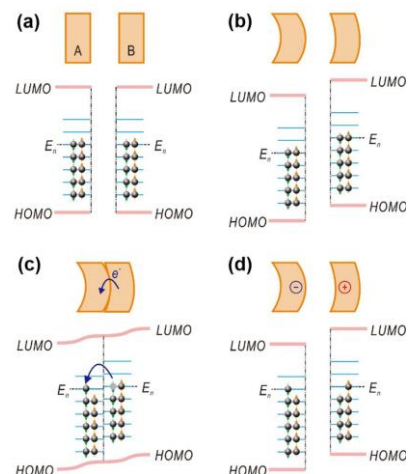
Figure 27. Identical materials with ideal flat surfaces (a) and different surface curvatures (b–d).

3.13.13. Ambient humidity. The charge between two materials is reduced upon the increase of humidity [6]. This possibly happens because of a conductive layer of water molecules which concentrate on their surfaces, thus conducting and leaking part of the created triboelectric charge. However, the role of humidity in contact charging is complex. Diaz et al. showed that for humidity less than 30%, the created triboelectric charges increase with the increase of humidity. Studying the effect of humidity became more confusing when Galembeck et al. found that a humidity change may drive to a change of the surfaces charges, prior to any contact between them [8].

3.13.14. Presence of air. The triboelectricity phenomenon happens in the air but we can observe it in vacuum conditions too. In this second case, the coming charge is often higher [6]. Further testing in a vacuum with polymers which were isolated from the air since their building has shown that the triboelectricity phenomenon still happens even for them [2].

3.14. TENGs developments

Thanks to the great research on TEGs, improved designs and material structures have brought numerous developments in different areas of applications. These areas are presented below, accompanied by some examples.

3.14.1. TENGs and water motion. Considering that the ocean wave energy is one of the most promising renewable and clean energy sources, Li et al. developed a nanowire-based TENG for harvesting wave energy as seen in Figure 29. Using nanowires on one of the surfaces he raised the contacting area with water and also made the polymer film hydrophobic (Figure 28). The outputs reached 10μA and 200V while keeping a low-cost,

41

chemical stability, lightweight, small size, and high efficiency even at low frequencies [29].
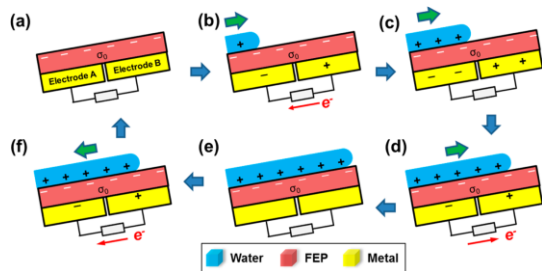
Figure 28. Electricity-generating process of the TEG by Zhu et al.
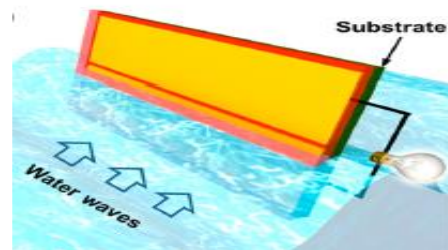
Figure 29. Schematic of the TEG positioned in water waves.
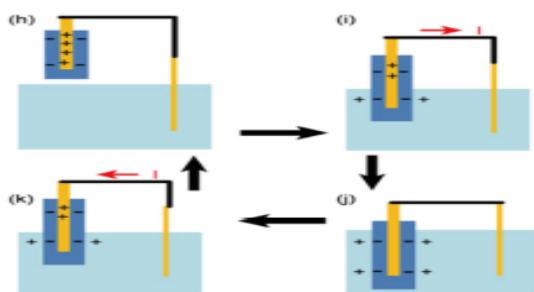
Figure 30. Electricity-generating process of the TEG by Li et al.
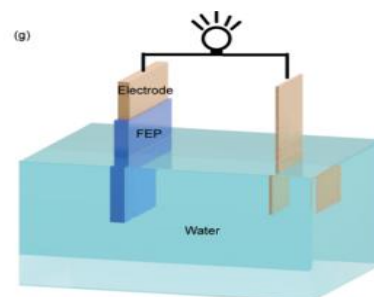
Figure 31. Schematic of the TEG positioned in water waves.

Zhu et al. developed a TEG which similarly works in water waves, thanks to the up-and-down movement of the surrounding water body (Figure 31) which induces electricity generated between two electrodes (Figure 30). It is expected that the use of nanowires on the surfaces can boost the electric outputs [47].

We must also mention the development of an integrated TENG for harvesting energy from rainwater by Liang et al. The instantaneous output power density reached 27.86mW/m² [48].

3.14.2. TENGs and air motion. A wind-rolling TENG was developed by Yong et al. It can generate electricity from wind as a lightweight dielectric sphere rotates along the vortex whistle substrate, thus producing a voltage of 11.2V and current of 1.86μA. However, the robustness and durability of the wind-driven TENGs pose challenges because of the wears caused by the friction and the load of the sphere's motion along the vortex [49].

Zhang et al. developed a flexible and transparent TENG made of free-standing polymer strips similar to a kelp forest [50]. The strips contact and separate during wind flow, no matter of the wind direction, contrary to other designs which work only under certain wind direction. Providing that the strip size was 10×2cm and airflow velocity 27m/s, two

adjacent strips with rooftop area of 2×0.7cm can offer voltage up to 98V, current of 16.3μA and power density of 2.76 W/m^{-2}.

3.14.3. TENGs and human motion. Wang et al. presented an integration of a flexible TENG with a flexible rechargeable Zn-ion battery system, embedded in a flexible 3D fabric, which could harvest energy from the human motion and store it to the battery using a rectifier circuit. The fabric TENG generated a voltage of 10–15V, a current of 3–4μAm and maximum output power 18.19mW/m^2 [51].

Hou et al. developed a simple and low-cost TENG to be placed in shoe soles and harvest human walking energy from weight during foot walking. The mechanism was based on the contact-separation mode between a polydimethyl sil-oxane (PDMS) film and a polyethylene terephthalate (PET) film. The maximum output voltage and current reached up to 220V and 40mA respectively [52].

Moreover, He et al. developed a smart textile by immersing a piece of cotton textile in a PEDOT:PSS solution, and used it to build a TEG, which can harvest energy from human stepping during walking or running [53]. The maximum output power density was 2W/m^2 (achieved from foot stepping at 2Hz on a layer of PEDOT:PSS coated textile of 4×4cm^2) [53].

Lin et al. built a TEG to harvest the energy of human walking and provide it to a wearable heart rate sensor, a wearable signal processing unit and a wearable Bluetooth module for wireless data transmission to a smartphone device. The maximum generated power reached 2.28 mW. It was also found that the voltage output increased from 200V to 540V with increasing of the external vibration frequencies from 6 to 10Hz [54].

3.14.4. TENGs and vehicle motion. The phenomenon of triboelectricity can also be met on the rolling tires during vehicle motion. When the electron-donating materials of the road surface (e.g. silica, cement) come in contact with electron-accepting materials of cars wheels (e.g. polymer or rubber), opposite charges can be induced on both surfaces. Mao et al. fixed a TENG on a rubber wheel, to examine the idea of harvesting this energy. This design imposes limitations as under real-world conditions the abrasion from the ground would quickly damage the functioning part. This challenge would be solved if the ground surface could act as one charge-generating material and the tire surface acts as the other one. Increase on the tire's rotation speed or load increased the voltage linearly in both cases [55].

3.14.5. TENGs and measuring. Bertacchini and Pavan used 3D printing and acetylic silicone (as the triboelectric material) to develop a low-cost TEG, used as a flowmeter of gases or fluids. A comparison between the output data of the TEG and a commercial flowmeter (used as reference) demonstrated the effectiveness of the device [56].

Interestingly, the nanowire-based TENG which Li et al. developed can be used not only as an energy generator but a chemical sensor as well. It was demonstrated that the

Μεταπτυχιακή Διπλωματική Εργασία, Αριστείδης Ρεπούλιας, ΑΜ 0014

current of the nanowire-based TENG decreased from 2.34μA to 0.4μA as the ethanol volume percentage in the liquid increased from 2.5% to 50% [29].

3.14.6. TENGS and rotational motion. A cylindrical rotating TENG was developed by Bai et al. based on the sliding charging mode to harvest mechanical energy from rotational motion [57].

Another two-dimensional rotary TENG was developed by Lin et al. This reached 0.75mA and 200V at a 500rpm rotating rate and a 750Hz frequency. Application examples of using this TENG is on the wheel of a bicycle or on a swinging human arm [58].

3.14.7. TEGs and sensoring. Considering the necessity of safe car driving and its close relation to the driver's seating position, a sensing system was built to monitor it and check if it is proper. Feng et al. attached two types of TEGs on a safety belt to monitor each moment the position and turnings of the driver's body [59].

Moreover Cao et al. combined conductive textiles and nanofiber membranes to build breathable and stretchable TEG structures for energy harvesting and biomechanical monitoring (e.g. respiratory monitoring) [60].

Another TEG based structure used to measure human joint motions and sweating behaviour was developed by Kiaghadi et al. under the name "Tribexor" [61].

Obstructive sleep apnea syndrome (OASA) is a respiratory disease caused by upper airway obstruction that is harmful to the quality of sleep and to human health. Thus Zhang et al. designed a 5x5cm^2 TEG structure which monitors the breathing status of human by sensing the variation of the abdomen circumference. It is based on the contact-separation mode, using as contact-pair a nylon film and a polytetrafluoroethylene (PTFE) film, plus copper foil sheets as the electrodes [34].

3.14.8. TEGs and medicals. Considering that there are various forms of power continuously released from our body (e.g. heartbeat, blood pressure, chest expansion through breathing or muscle movements etc) it is becoming clear that developing appropriate TEGs to harvest this energy, might support pacemakers, cardiac or breathing monitoring etc [22].

An interesting example comes from Ouyang et al. who developed a TENG to harvest the energy motion of the heart and power an implanted pacemaker instead of the bulky, rigid and short-lifetime pacemaker batteries [62]. The TENG was placed between the heart and pericardium so that periodic and continuous contact and separation was applied between its two surfaces. A 100μF capacitor was added to store the electrical energy through a rectifier. The capacitor's voltage could rise from zero to 3.55V into 190min when having ~100/70mmHg blood pressure and ~77bpm heart rate. The TEG's voltage reached ~65.2V and current ~0.5μA, while it harvested 0.495μJ from every cardiac motion which covers the necessary demands of endocardial pacing (0.377μJ).

Wang et al. demonstrated a biomedical TENG, which uses a biocompatible medical 317L stainless steel plate and an ethyl cellulose film as the two contacting surfaces, plus

silver wires as electrodes. The voltage output reached 245V and the current 50mA. The performance of the TEG was tested by immersing it in simulated body fluid for a month and showed that it didn't change obviously, thus revealing that it shows biocompatibility and great potential for applications in biomedical science [63].

4. Issues

Practically, the study, measurement, development or manufacture of TEGs show a number of issues. These problems and their possible solutions are explained below.

4.1. Voltage and current measurements

A common issue in developing or studying TEGs is the accurate measurement of their low electrical current [9]. The high resistance of the TEG plus that of the oscilloscope (which is used to preview the phenomenon) reduces te electrical outputs. Especially for electrical current, it is difficult to measure it without disturbing it [9].

The simplest solution for measuring TEG's output electrical current is to connect a resistive load to the TEG, measure the voltage across the resistor, and calculate the electrical current using apply Ohm's law (I = V/R). Although this seems to be theoretically right, a few problems prevent its practical application because of possible occurring noise in the signals, thus driving to not correct measurements [9].

A solution for the accurate electrical current output measurement comes from the use of a preamplifier, which is unfortunately pretty expensive and is considered as an obstacle for the new research entrants. Nevertheless, Malinelli et al have developed and presented the use of a cost-effective circuit which can replace the expensive preamplifiers without any significant difference in measurements [9].

4.2. Conversion of voltage

We must keep in mind that regular mobile electronics need usually 3.3-5V to operate, plus tens or hundreds of mA of current. On the other hand, TEGs can produce a voltage of a range of hundreds of volts and a current of few μA. So the use of special converters is applied for the conversion of voltage [3].

4.3. Long stops of charging

Moreover, if there are long stops on the mechanical movement of the TEG's sheets (e.g. because of human resting after an exercise), mobile electronics which are self-feed by TEGs will need a backed-up power source to keep operating (e.g. a battery). In this case, the use of special electronic circuits is required [3].

4.4. The limited direction of mechanical movement

Many TEGs have been developed but most of the times the direction of their mechanical movement is restricted to only one. Therefore the development of TEGs which do not depend on the direction of mechanical movement is of high interest in the market [3].

4.5. Production's high demands

Finally, considering the production demands of TEGs, it is very important to keep its manufacture at a low cost and the device's reliability and robustness at a high level, not forgetting to keep it all environmental-friendly [11]. Another demand is to keep it maintenance-free [58].

4.6. Durability

Finally, another crucial prerequisite for the TEG designs when attached to clothes etc is their continuous exposure to high-stress conditions. Thus they must be resilient to deformation or cracking, water-resistant when being washed etc [15]. So testing their durability by running them for numerous operation circles is necessary.

4.7. Comfortability

Moreover, a big challenge is the need for achieving comfortability for the wearable TEGs. As polymer materials in the film's form are not breathable, they may cause discomfort and even possible inflammation to the wearer. The solution to this problem is achieved by integrating TEGs into skin-friendly textile fabrics [15,19].

5. The goal of this study

After the current generic introduction to triboelectricity, the next chapters focus on the main goal which is the study and comparison of the triboelectric outputs for a number of textile structures. To achieve this goal, the reproduction and testing of the triboelectric phenomenon under controllable conditions through the development of a prototype testing device were applied.

Μεταπτυχιακή Διπλωματική Εργασία, Αριστείδης Ρεπούλιας, ΑΜ 0014

6. Concept

The study of how textile fabrics can perform in the triboelectric phenomenon and the comparison of different textile fabrics under the same conditions rises an interest, in a period that a lot of research is applied on the TENGs development to be used for energy harvesting or self-powered sensors.

In order to study the way that the triboelectric outputs are affected by the contact time duration of the fabrics, the force applied between the fabrics, the contact surface depending on the oriented positions of the fabrics, and the surface patterns, certain testing measurements were needed. So it would be necessary to reproduce the phenomenon in a real environment under controllable conditions and make the appropriate tests and measurements.

To achieve this, a prototype testing device was designed and developed, which allowed us to measure different samples under the same conditions or the same sample under different conditions. The device's operation concept was to have two flat electrodes where the textile samples would be placed, to tap them controllably and accurately by an adjustable control unit and to record the outcoming voltage values with the support of another electronic means so that the measurements might be processed later. Considering that the tapping frequency and the tapping force could be adjustable, the testing conditions would be to a large extent controllable.

7. Chosen method

Following the theory of the previous chapter, the testing device had to execute one of the four triboelectricity modes. The finally chosen method was the vertical contact-separation mode, being the simpler one to reproduce with high accuracy. To keep it simple was important in order to avoid undesired structural defects or side effects which might provide mistaken measurements as the measured values would be very low.

The experiment to study if there is an effect on the electrical outcomes from changing the fabrics surfaces orientations during their contact, was based on applying tests to record measurements of pairs of woven fabric samples with one of them being manually turned at four different angles positions: at -90°, 0°, 90° and 180°.

In order to compare the electric outcomes of different textile surface patterns of the same material, textile fabric samples with different surface patterns on each of their side were used.

To study the effect of different forces during the contact of textile samples, we applied experiments to record the electrical outputs of pairs of woven fabric samples for various tapping forces. Then a representation of the electrical outputs and forces was made to show if there is a relation between them.

Finally, an experiment was designed to study the influence of the contact time duration of the textile fabric samples. We applied experiments to record the electrical outputs of pairs of woven fabric samples under various time durations of tapping.

8. Required mediums

Apart from the new prototype testing device, a few extra mediums were necessary to achieve our goal. So in order to measure the electrical output coming from the contact of textile fabrics, a digital oscilloscope was used. This was connected to a laptop to download the measured data in the desired formats (as values or image graphs).

Moreover, two codings were used: one for controlling the times of tapping of the two samples and another to measure the weight applied at the moment of the contact. We used C++ language and the Arduino Integrated Development Environment (Arduino IDE). Each of the two codings was assigned to an Arduino board (a single-board microcontroller for building digital devices) so that the codes would be executed continuously and independently. Thus two Arduino boards were required.

A weighing sensor was also used to measure the weight applied between the two textile fabrics at the moment of their contact. Its analogue values were transformed into digital and previewed to a laptop. The measured weight values were converted into force later.

Finally, the use of a dimmer resistance in the power supply circuit of the tapping mechanism was necessary to gradually reduce the applied force during the samples contacts.

9. Measuring mediums

An oscilloscope was used to measure the TEG's voltage (V maximum, V peak to peak and V average). Because measurements of electrical current were not applied, no preamplifier was used and no resistive load was connected to the TEG.

The oscilloscope's model was Agilent Technologies DSO3102A. It is a digital one, with an input impedance of 1MΩ and capacitance of ~13pF. Automatic calibration and self-test were applied before the application of measurements.

The probes model was the Agilent N2862A. These are 10:1 probes, with an input impedance of 10MΩ and a capacitance of 15pF. The probes were calibrated following the appropriate procedure with the oscilloscope's 3V signal generator.

10. Quick presentation of the device

In order to study and demonstrate the phenomenon of triboelectricity through different textile samples, and study the external parameters of contact time, contact force, contact positioning and contact surface, a controllable and adjustable TEG obeying to the vertical contact-separation mode as seen in Figure 32 was built. This TEG testing device was the main element of the measuring system presented in Figure 33.
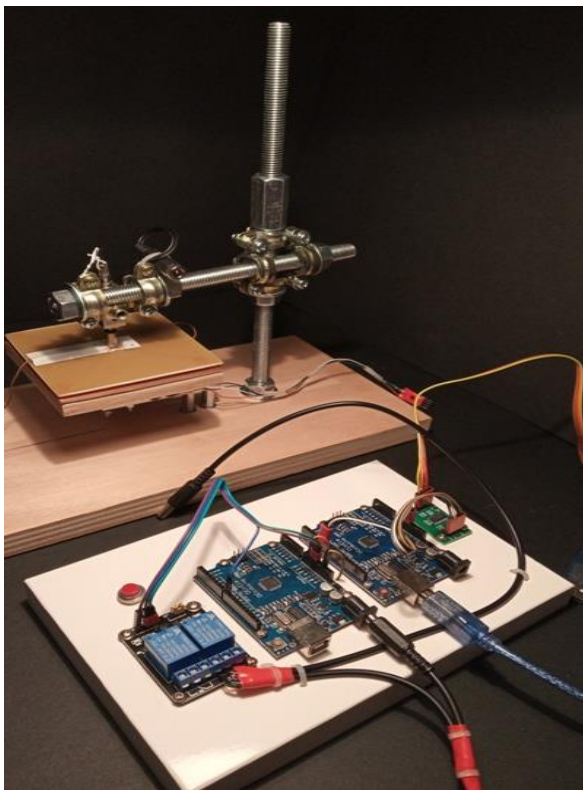
Figure 32. The prototype TEG testing device.

Figure 33. The complete testing system.

11. Main demands of the device's operation

The maximum precision was the number one priority. Considering the really low values of voltages which are instantly produced in TEGs, it was a prerequisite to attain high precision, reliability and repeatability during the experimental process. The maximum voltages (V_{max}) needed to be recorded so that we may compare the electrical outputs of the tested samples.

Μεταπτυχιακή Διπλωματική Εργασία, Αριστείδης Ρεπούλιας, ΑΜ 0014

The second demand to look after was the ability of the operator to adjust the time-related parameters, like the time duration of the contact, the idle time, the contact frequency and the number of repeats. This way we could study their effect on the electrical outputs of the samples under the desired time conditions.

Moreover, a third one was the ability to place and measure samples of different thickness, keeping in mind that textile fabrics have various thicknesses.

Finally, we needed to know the exact applied force on the samples surfaces during each contact, so that we could have a complete awareness of the testing conditions. Keeping this force adjustable might let the operator to better control the testing conditions.

12. Main decisions for the device's design and development

While designing the testing device, keeping in mind the before mentioned operational demands and the goal of keeping it simple, efficient and precise, the following main decisions were taken:

- Electrodes must have high conductivity to capture and transfer the generated low electrical outputs with minimum loss. Aluminium foil was rejected as it doesn't osculate steadily, so the use of copper sheet (FR4) was chosen.
- Good surface contact must be achieved between the samples at the contact moment.
- The samples must be positioned easily on the electrodes.
- Both the samples and the electrodes must be electrically isolated from the rest of the frame so that there is no interferes or loss in signals.
- One of the electrodes must be able to turn 360° so that we may test fabrics under different orientations.
- The distance of the electrodes shall be adjustable so that thick or thin samples could be placed on them keeping a constant air gap of about 3mm between them.
- The contact time duration of the samples must be easily adjustable so we may try various testing settings.
- The idle time duration till the next samples contact must be easily adjustable so we may try various testing settings.
- The number of contact repeats must be easily adjustable thus permitting various testing settings.
- The applied force between the two electrodes must be adjustable to control the testing conditions.
- Attention must be taken into account in eliminating any noise signals in the testing system.
- The building cost shall be kept low and the construction as simple as possible.

13. Development steps

13.1. *Step 1 – Development of the frame*

In order to provide static stability and insulation, a thick plywood piece (17x28x2cm) was used as the device's base. A threaded rod of 30cm length and 11mm diameter (called the vertical arm) was attached vertically on it through a drilled hole. Nuts and rings were used to fix it properly.

Another piece of threaded rod of 20cm length and 11mm diameter (called the horizontal arm) was attached perpendicularly on the vertical one (Figure 34). The connection was achieved by using pipe clamps for wall mounting, in combination with nuts. This link permits the operator to turn round 90° the horizontal arm, resulting in adequate space for changing the samples. Moreover, it permits the operator to displace the horizontal arm lower or higher if turning it 360° clockwise or anticlockwise respectively. The scenario of a compact and permanent connection between the two arms was rejected as in that case it would prevent the two before mentioned crucial abilities.

Finally, the metal frame (Figure 35) was earthed with the use of an appropriate cable connection.
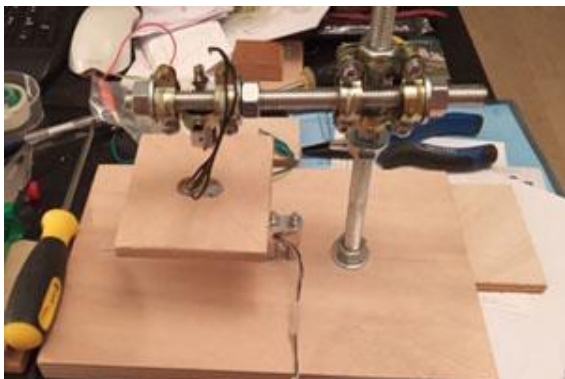
Figure 34. View of the frame.

Figure 35. Connection of the arms.

13.2. *Step 2 – Development of the electrodes*

Each of the two electrodes was developed using FR4 boards (1mm thick) with a copper coating on one of its two sides (Figure 36). Both of the FR4 electrodes were rectangular, with surface dimensions of 9.5x9.5cm. A small hole was drilled carefully on the centre of each FR4 board. Afterwards, a thin cable was inserted into that hole, with direction from back to the front of the FR4 board and it was soldered (Figure 37). Finally, the excessive soldering of the joint on the front side was smoothened with a Dremel tool (Figure 38) so that it doesn't protrude.

On one of the two FR4 electrodes, a double side adhesive tape was attached at its non-conductive side (Figure 39). In step 3 this would be attached to the weighing sensor's plywood plate.

On the second FR4 electrode, an appropriate female to female PCB spacer (PCB standoff) was attached with glue at the centre of its non-conductive side. This would be used to fasten the electrode on the solenoid's moving shaft in step 4.

Figure 36. Cutting the FR4 board.

Figure 37. Soldering the FR4.

Figure 38. Finishing the soldering.

Figure 39. Back side of FR4 and its base.

13.3. Step 3 – Development of the weighing mechanism

To measure the weight applied between the samples at the moment of the contact, a 1000gr commercial weighing cell (bridge sensor) was used, supported by a 24-bit analog to digital converter (model HX711). Later the weight values would be converted to force.

Appropriate screws, bolts and spacers (PCB standoffs) were added on the weighing cell's sockets (Figure 40). The lower extension-screws of the weighing cell fastened onto the device's plywood base. The upper extension-screws of the weighing cell fastened onto a plywood plate of the same dimensions as the FR4 electrodes (9.5x9.5cm). Finally, the previous step's FR4 electrode (with the double-sided adhesive tape), was attached to this plywood plate (Figure 41).

Concerning the signals transfer, the weighing cell connected to the HX711 module, the HX711 connected to an Arduino board, and the Arduino board connected to a laptop to view the running values through a serial monitor panel.
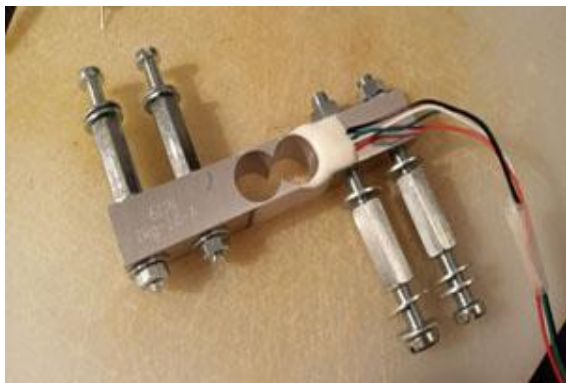
Figure 40. Weighting sensor.
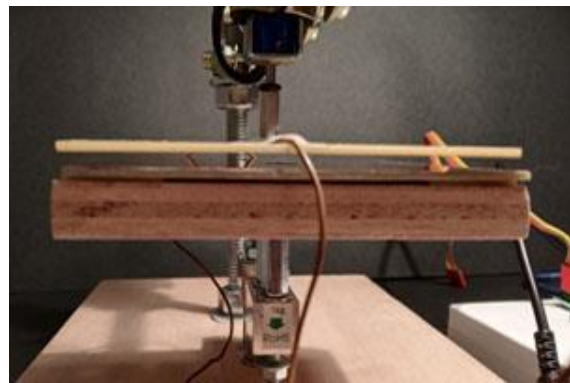
Figure 41. View of the position of weighting sensor.

In order to make the weighing cell to work properly, three steps had to be followed. First, a necessary library was uploaded to the Arduino board. Secondly, an appropriate sketch was uploaded for the calibration of the cell readings. And finally, another was uploaded for getting and previewing the measurements.

13.4. Step 4 – Development of the tapping mechanism

In order to bring in contact the textile samples and reproduce the vertical contact and separation mode, the commercial DS-0420S electromagnetic solenoid was used. This is a push-type solenoid using 12V DC to activate. It was externally insulated and attached on the horizontal arm of the device's frame using pipe clamps for wall mounting (Figure 42).

The solenoid's activation was controlled by an electrical relay, which opened or closed the circuit of 12V DC power coming from a PS1.3-12 battery (12V, 1.3Ah). Further on, the relay activation was connected to an Arduino board (Figure 43) after uploading an appropriate sketch and setting the desired time parameters. A restart button was added to the Arduino to let the tapping mechanism begin a test by simply pressing it.
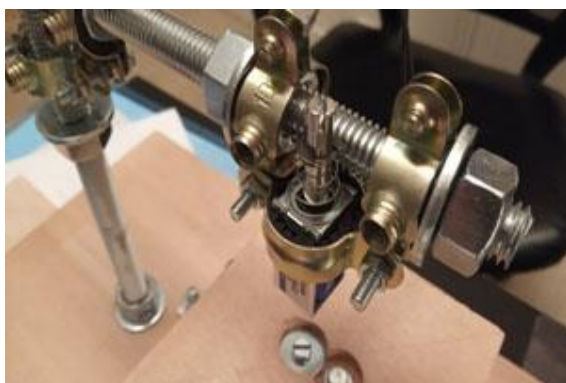
Figure 42. Solenoid tapping mechanism.
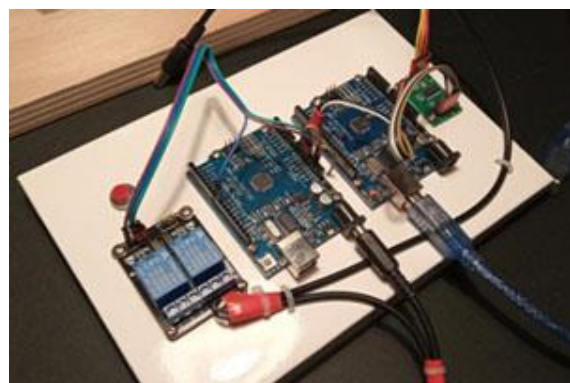
Figure 43. Arduino boards control units.

The parameters which can be set anytime from the operator regarding the solenoid's activation are: (i) the contact time duration in milliseconds (Time1), (ii) the idle time duration until the next contact in milliseconds (Time2), and (iii) the number of repeats (TestNr). Finally, the electrode with the attached female to female PCB spacer (PCB standoff) was fastened to the solenoid's moving shaft. The cablings of the tapping and weighing mechanism are shown in Figure 44.
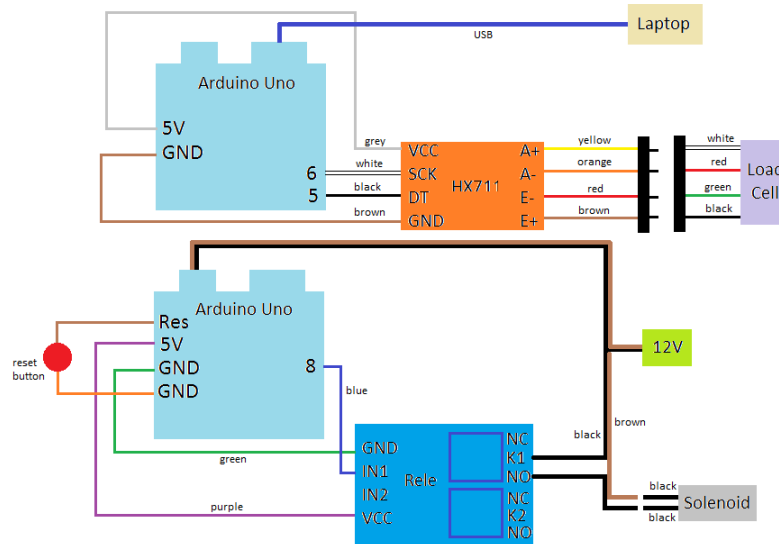
Figure 44. Draw of the electronic connections of the tapping and weighing mechanisms.

13.5. *Step 5 – Additional actions*

An oscilloscope (specifications mentioned in the previous chapter) was used to measure the testing device's coming voltage (Vmax). The display's vertical axe (CH1) was set to 1 or 2 V/div, and the horizontal axe was set to 2000Sa/s sampling. The trigger action was set to normal and simple (not auto) mode with a threshold of 80mV to capture and freeze the preview of the detected signals.

A dimmer resistance was connected between the battery and the solenoid so that the power supply could be adjusted to allow various tapping force values during the samples contact.

To eliminate any noise signals coming from the peripheral electrical equipment of the testing system (laptops, power supply cables etc), the testing device was placed on a wooden stool.

Concerning the power supply of the solenoid, the use of a 220V AC to 12V DC transformer was rejected because it was causing continuous noise which was then captured from the electrodes. A commercial battery of PS1.3-12 type (12V, 1.3Ah) was used instead to solve this issue.

In a similar case, as for the power supply of the two Arduino boards, the use of 220V AC to 12V DC transformer was rejected because it was causing continuous noise too. So

they got power from a laptop's USB ports. The same laptop was used for accessing and adjusting the solenoid's tapping settings and preview the weighing measurements too.

Attention was taken so that the solenoid's shaft does not extend to the maximums when activated, otherwise it hits the solenoid's frame causing a noisy mechanical shock to the attached electrode and mistaken signals respectively.

13.6. *Step 6 – Confirmation of correct performance*

After building the electrodes and before their installation on the device's frame, their performance was tested manually. The phenomenon was reproduced by adding textile samples on the electrodes and tap them manually while being connected to the oscilloscope. In order to avoid charge interference caused by the fingers while tapping the samples, insulated grips were added on their back temporarily. Upon their contact, the phenomenon was correctly reproduced, no matter of the electromagnetic solenoid's absence.

Moreover, to exclude the scenario that the FR4 electrodes just capture environmental radiation, these were also tested in an electromagnetically isolated anechoic chamber. The vertical contact-separation triboelectric phenomenon was successfully reproduced, thus confirming that the oscilloscope's readings are not coming from environmental noise capture but from the triboelectricity phenomenon.

A number of different tests were also carried out after building the testing device to confirm that the signals received from the contact of the samples were not a result of interferences from the device's metal frame, cables or the solenoid. Trials were carried out without power in the connection cables, without power in the solenoid, and without samples on the electrodes. In all the cases it was clear that they do not influence the oscilloscope's readings.

The weighing mechanism was confirmed for measuring correctly by placing a certified 50gr calibration weight after execution of the calibration process.

Finally, the time accuracy of the relay's and solenoid's activations was checked. To do this, a tapping of the samples with 1Hz for 10 repeats was applied. The voltage signals were recorded in the oscilloscope and downloaded. The coming data sheet was processed knowing that oscilloscope's sampling was 1000samples/sec. After counting the recorded values between the voltage peaks, it was found that every 1000±1 values there was a peak, thus confirming that the solenoid's activation period was very precise.

Μεταπτυχιακή Διπλωματική Εργασία, Αριστείδης Ρεπούλιας, ΑΜ 0014

14. Preparation of testing

The tapping system's (solenoid) power supply was connected to the relay module, while the relay module was connected to the battery. The weighing system (weighing sensor) was connected to the HX711 module. To preview the weighing measurements, a laptop was connected to the Arduino which controls the weighing system. The laptop was also connected to the Arduino which controls the tapping system to set the tapping parameters. Finally, the oscilloscope's probe was connected to the electrodes and to a laptop to preview online and download the measurements.

15. Preparation of samples

Each sample was cut appropriately at 11.5x9.5cm and positioned to cover firmly the conductive surface of each electrode. It was held on the electrode by folding its two longest sides (11.5cm) and sticking them with some adhesive tape on the electrode's non-conductive backside. Therefore each sample's exposed surface at the moment of the contact was equal to the electrode's dimensions (9.5x9.5cm). The selected textile fabric samples are presented in Table 1 below:

Table 1. Characteristics of the selected textile fabric samples.

Sample	Structure form	Thickness (mm)	Weight (g/m²)
PES100%	plain woven fabric	0.35	120
COT66%-PES34%	plain woven fabric	0.25	85
COT100%	plain woven fabric	0.20	100
WOOL100%	plain woven fabric	0.35	115
COT100% wafer	wafer woven fabric	0.40	125
COT100% velvet	velvet woven fabric	0.35	130

Detailed images of the textile fabric samples with an inserted reference ruler of 1cm length are consecutively presented from Figure 45 to Figure 52.

Μεταπτυχιακή Διπλωματική Εργασία, Αριστείδης Ρεπούλιας, ΑΜ 0014
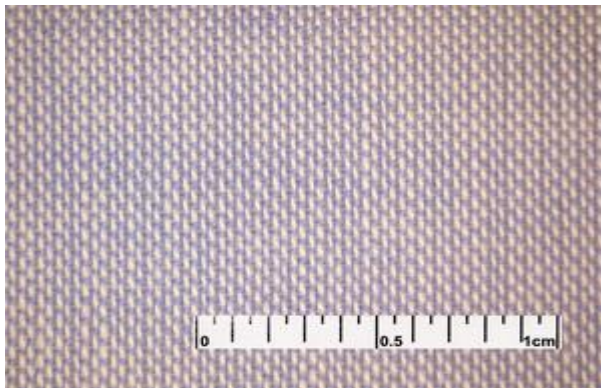
Figure 45. The COT100% sample.
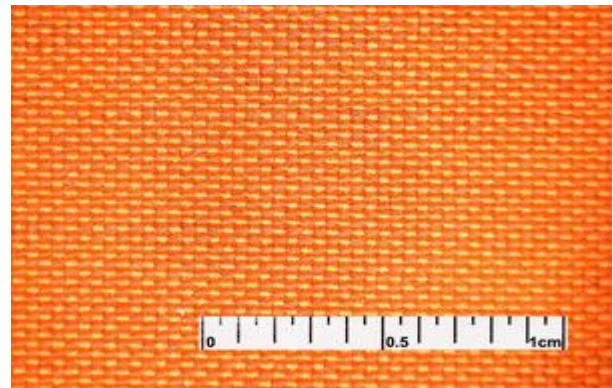
Figure 46. The COT66%-PES34% sample.
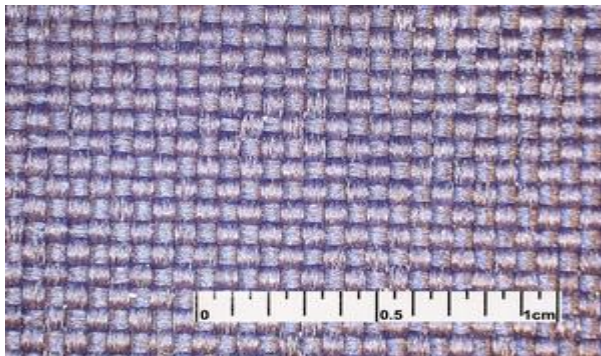
Figure 47. The PES100% sample.

Figure 48. The WOOL100% sample.
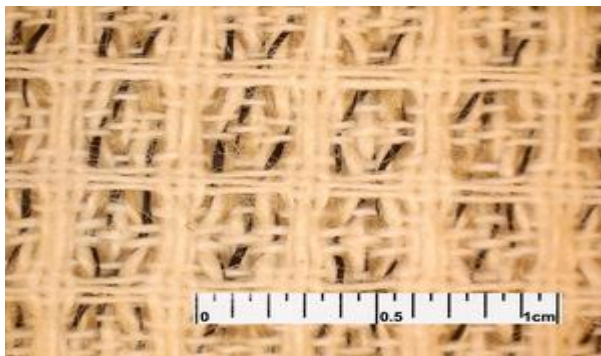
Figure 49. The COT100% wafer sample (Side A).
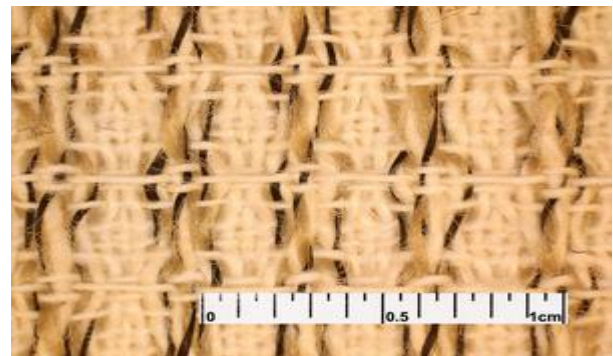
Figure 50. The COT100% wafer sample (Side B).

Figure 51. The COT100% velvet sample (piled side).
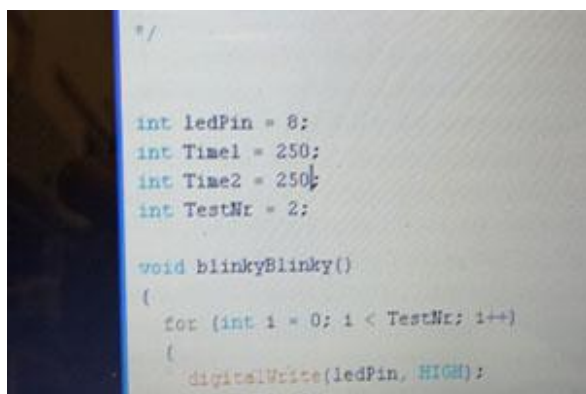
Figure 52. The COT100% velvet sample (plain side).

57

16. Procedure for testing

The procedure of testing starts by setting in the tapping system the desired (i) contact time duration in milliseconds (Time1), (ii) idle time duration until the next contact in milliseconds (Time2), and (iii) number of repeats (TestNr) as seen in Figure 53. A contact time of 200ms (Time1=200ms) was recommended for the weighing system to record sufficiently the applied contact force. During the tests, single contacts were applied between the samples surfaces, meaning one tapping per test (TestNr=1).
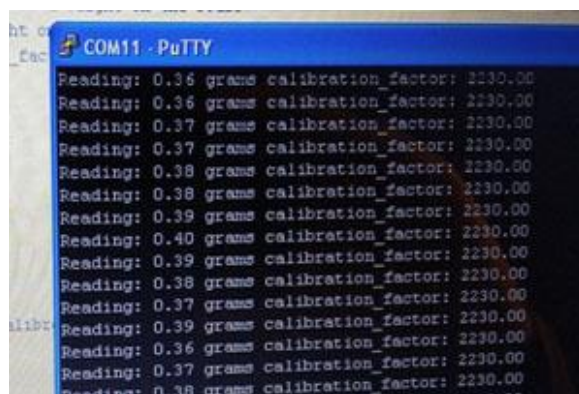
The oscilloscope is then set. As mentioned before, the display settings are set to measure the testing device's coming voltage and also record the V_{max} value. The vertical axe of the display (CH1) was set to 1 Volt/div, and the horizontal axe was set to 2000Sa/s sampling. The trigger action was set to single and normal (not auto) mode, with an 80mV threshold in order to capture and freeze the preview of the measurements. In order to exclude any possible deviations due to hardware issues during the tests, the same oscilloscope channel (CH1) and probe were used.

Figure 53. View of tapping mechanism settings as seen in Arduino IDE.

Figure 54. View of weighing readings as seen in a terminal window.

In the continue, the samples are placed on the electrodes (Figure 55) with the support of adhesive tape as was described before and the distance between the samples is checked and recorded (Figure 56). If there is no air gap of 3mm between the samples (because any of them is thick) then we must move the upper electrode higher. This is achieved by turning anti-clockwise the device's horizontal arm around the vertical threaded rod, thus displacing it higher.

The next thing to check is to turn on the display of the weighing values using a connected laptop's terminal window and to record the maximum weight measurements (W_{max}) which appear at the contact moment (Figure 54). The weighing sensor must be calibrated. We verify this by weighing a 50gr calibration weight. We must mention that the system's sensor measures mass, so we initially record these values in their original form (gr), as seen in the analytical measurements tables. Though, in the final tables we converted them to force (N).

58

Μεταπτυχιακή Διπλωματική Εργασία, Αριστείδης Ρεπούλιας, ΑΜ 0014

After completing these procedures, we can push the button to restart the tapping system's operation for a testing cycle. The contact of the samples is being performed at that point and the result presented on the oscilloscope. We download the recorded values from the oscilloscope to the connected laptop to save them. We then repeat the testing procedure by pushing the restart button again.

During the testing, all the voltage signals were recorded, but only maximum voltage (V_{max}) was used for the study.
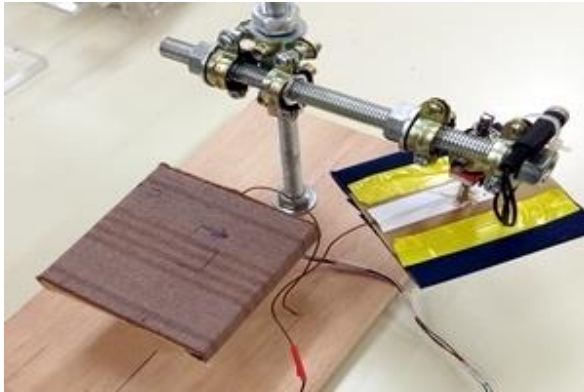
Figure 55. Position of two electrodes (with attached samples) while preparing the test.
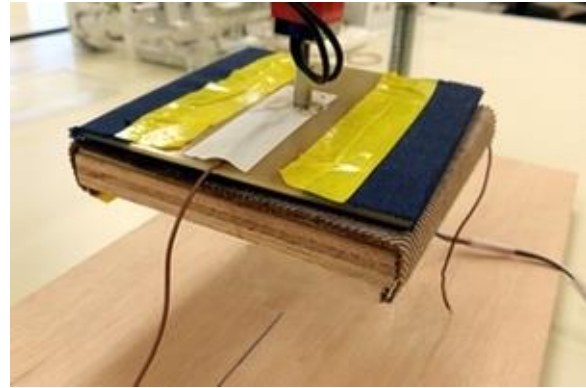
Figure 56. Position of two electrodes (with attached samples) during the test.

17. Testing conditions

The ambient testing conditions in the laboratory were $20\pm2°C$ and $65\pm2\%$ RH (following the standards for textile testing). Prior to their testing, samples stayed 24 hours in the laboratory.

18. Test results

18.1. *Test results for different orientations of the samples surfaces during their contact*

To change the orientation of the two samples surfaces during their contact, one of the two samples was rotated 90° for each group of measurements (the one attached to the solenoid shaft) while the other sample was steady (the one attached on the weighing sensor). The recorded measurements are presented analytically in the tables below, from Table 2 to Table 9. Contact time and contact force were constant.

Initially, pairs of same textile fabrics were selected: two identical samples of COT100%, two identical samples of COT66%-PES34%, two identical samples of WOOL100%. Because these sample pairs show negligible voltage output, only a few measurements were enough to be applied. Moreover, two identical samples of PES100% were tested.

Μεταπτυχιακή Διπλωματική Εργασία, Αριστείδης Ρεπούλιας, ΑΜ 0014

In the continue, pairs of different textile fabrics were selected: COT66%-PES34% with WOOL100%, PES100% with WOOL100%, PES100% with COT66%-PES34%, and PES100% with COT100%.

Table 2. Orientation test for two identical COT100% woven fabrics*.

Angle	0º		-90º		90º		180º	
	W_{max} (gr)	V_{max} (V)	W_{max} (gr)	V_{max} (V)	W_{max} (gr)	V_{max} (V)	W_{max} (gr)	V_{max} (V)
Test 1	106	0.16	100	0.16	99	0.16	104	0.16
Test 2	107	0.16	101	0.16	100	0.16	103	0.12
Test 3	106	0.16	101	0.16	100	0.16	104	0.16
Test 4	106	0.16	101	0.16	99	0.16	106	0.16
Test 5	107	0.20	101	0.16	99	0.16	106	0.16
Average	106	0.17	101	0.16	99	0.16	105	0.15
STD	0.55	0.02	0.45	0.00	0.55	0.00	1.34	0.02
CV	0.51	10.65	0.44	0.00	0.55	0.00	1.28	11.77

*Distance: 3mm / Contact time: 200ms

Table 3. Orientation test for two identical COT66%-PES34% woven fabrics*.

Angle	0º		-90º		90º		180º	
	W_{max} (gr)	V_{max} (V)	W_{max} (gr)	V_{max} (V)	W_{max} (gr)	V_{max} (V)	W_{max} (gr)	V_{max} (V)
Test 1	82	0.16	82	0.20	94	0.20	90	0.16
Test 2	83	0.16	82	0.20	93	0.16	90	0.20
Test 3	85	0.16	82	0.12	93	0.12	90	0.16
Test 4	83	0.20	85	0.12	93	0.16	88	0.16
Test 5	82	0.16	85	0.12	94	0.12	88	0.16
Average	83	0.17	83	0.15	93	0.15	89	0.17
STD	1.22	0.02	1.64	0.04	0.55	0.03	1.10	0.02
CV	1.48	10.65	1.97	28.83	0.59	22.02	1.23	10.65

*Distance: 3mm / Contact time: 200ms

Table 4. Orientation test for two identical WOOL100% woven fabrics*.

Angle	0º		-90º		90º		180º	
	W_{max} (gr)	V_{max} (V)	W_{max} (gr)	V_{max} (V)	W_{max} (gr)	V_{max} (V)	W_{max} (gr)	V_{max} (V)
Test 1	108	0.16	109	0.24	101	0.16	115	0.24
Test 2	104	0.24	102	0.24	99	0.16	122	0.16
Test 3	106	0.24	103	0.16	99	0.16	122	0.16
Test 4	107	0.24	109	0.24	95	0.24	118	0.24
Test 5	108	0.16	108	0.16	96	0.24	124	0.24
Average	107	0.21	106	0.21	98	0.19	120	0.21
STD	1.67	0.04	3.42	0.04	2.45	0.04	3.63	0.04
CV	1.57	21.07	3.22	21.07	2.50	22.82	3.02	21.07

*Distance: 3mm / Contact time: 200ms

Μεταπτυχιακή Διπλωματική Εργασία, Αριστείδης Ρεπούλιας, ΑΜ 0014

Table 5. Orientation test for two identical PES100% woven fabrics*.

Angle	0°		-90°		90°		180°	
	W_{max} (gr)	V_{max} (V)	W_{max} (gr)	V_{max} (V)	W_{max} (gr)	V_{max} (V)	W_{max} (gr)	V_{max} (V)
Test 1	95	3.36	94	3.36	91	3.20	95	3.36
Test 2	94	3.36	94	3.36	95	3.36	95	3.44
Test 3	95	3.36	90	3.20	91	3.28	95	3.44
Test 4	95	3.36	91	3.20	92	3.20	91	3.36
Test 5	96	3.44	91	3.20	95	3.36	95	3.36
Average	**95**	**3.38**	**92**	**3.26**	**93**	**3.28**	**94**	**3.39**
STD	0.71	0.04	1.87	0.09	2.05	0.08	1.79	0.04
CV	0.74	1.06	2.03	2.68	2.21	2.44	1.90	1.29

*Distance: 3mm / Contact time: 200ms

Table 6. Orientation test for COT66%-PES34% and WOOL100% woven fabrics*.

Angle	0°		-90°		90°		180°	
	W_{max} (gr)	V_{max} (V)	W_{max} (gr)	V_{max} (V)	W_{max} (gr)	V_{max} (V)	W_{max} (gr)	V_{max} (V)
Test 1	113	0.16	110	0.24	115	0.16	110	0.24
Test 2	116	0.24	115	0.16	114	0.24	111	0.17
Test 3	110	0.24	113	0.16	120	0.24	110	0.16
Test 4	112	0.24	110	0.24	120	0.16	113	0.24
Test 5	112	0.16	110	0.16	122	0.24	115	0.24
Average	**113**	**0.21**	**112**	**0.19**	**118**	**0.21**	**112**	**0.21**
STD	2.19	0.04	2.30	0.04	3.49	0.04	2.17	0.04
CV	1.95	21.07	2.06	22.82	2.96	21.07	1.94	19.63

*Distance: 3mm / Contact time: 200ms

Table 7. Orientation test for PES100% and WOOL100% woven fabrics*.

Angle	0°		-90°		90°		180°	
	W_{max} (gr)	V_{max} (V)	W_{max} (gr)	V_{max} (V)	W_{max} (gr)	V_{max} (V)	W_{max} (gr)	V_{max} (V)
Test 1	76	3.36	74	3.44	76	3.04	77	3.68
Test 2	74	3.52	74	3.44	72	3.20	80	3.68
Test 3	72	3.52	72	3.36	70	3.20	81	3.68
Test 4	77	3.52	74	3.44	80	3.52	75	3.52
Test 5	77	3.60	75	3.44	77	3.52	75	3.44
Test 6	79	3.60	72	3.36	76	3.52	76	3.44
Test 7	79	3.52	80	3.52	74	3.36	74	3.36
Test 8	79	3.52	76	3.44	76	3.44	75	3.44
Test 9	76	3.52	73	3.36	77	3.52	76	3.52
Test 10	75	3.52	72	3.36	80	3.60	75	3.52
Average	**76**	**3.52**	**74**	**3.42**	**76**	**3.39**	**76**	**3.53**
STD	2.32	0.07	2.44	0.05	3.16	0.19	2.32	0.12
CV	3.04	1.86	3.29	1.58	4.16	5.47	3.04	3.29

*Distance: 3mm / Contact time: 200ms

Table 8. Orientation test for PES100% and COT66%-PES34% woven fabrics*.

Angle	0°		-90°		90°		180°	
	W_{max} (gr)	V_{max} (V)	W_{max} (gr)	V_{max} (V)	W_{max} (gr)	V_{max} (V)	W_{max} (gr)	V_{max} (V)
Test 1	75	2.00	73	1.92	62	1.80	65	2.04
Test 2	77	2.08	75	1.80	66	1.84	64	2.00
Test 3	72	2.04	75	1.76	66	1.84	62	1.92
Test 4	74	1.92	64	1.72	67	1.84	65	1.92
Test 5	75	2.00	66	1.76	66	1.76	64	1.92
Test 6	75	2.00	65	2.08	64	1.84	70	2.00
Test 7	68	1.92	67	1.84	64	1.92	71	2.00
Test 8	57	1.88	71	1.84	65	1.92	71	2.04
Test 9	77	2.08	67	1.84	66	1.92	71	2.04
Test 10	65	2.08	64	1.84	67	1.92	72	2.00
Average	**72**	**2.00**	**69**	**1.84**	**65**	**1.86**	**68**	**1.99**
STD	6.40	0.07	4.40	0.10	1.57	0.06	3.81	0.05
CV	8.95	3.65	6.40	5.52	2.40	3.08	5.64	2.52

*Distance: 3mm / Contact time: 200ms

Table 9. Orientation test for PES100% and COT100% woven fabrics*.

Angle	0°		-90°		90°		180°	
	W_{max} (gr)	V_{max} (V)	W_{max} (gr)	V_{max} (V)	W_{max} (gr)	V_{max} (V)	W_{max} (gr)	V_{max} (V)
Test 1	73	2.64	70	2.56	71	2.56	70	2.64
Test 2	73	2.64	71	2.64	72	2.56	70	2.64
Test 3	73	2.64	71	2.60	71	2.64	69	2.64
Test 4	74	2.60	71	2.64	72	2.60	70	2.64
Test 5	74	2.64	71	2.64	70	2.64	69	2.68
Test 6	65	2.68	65	2.60	72	2.56	69	2.64
Test 7	64	2.64	64	2.64	72	2.64	69	2.68
Test 8	64	2.64	64	2.56	72	2.64	69	2.64
Test 9	65	2.64	69	2.56	72	2.68	69	2.68
Test 10	65	2.56	69	2.64	71	2.72	68	2.64
Average	**69**	**2.63**	**69**	**2.61**	**72**	**2.62**	**69**	**2.65**
STD	4.67	0.03	2.99	0.04	0.71	0.05	0.63	0.02
CV	6.76	1.20	4.37	1.41	0.99	2.06	0.91	0.73

*Distance: 3mm / Contact time: 200ms

18.2. *Test results for different contact forces between the samples surfaces*

To study the results of different forces between the samples surfaces during their contact, one of the two samples tapped on the other with various controllable force but constant contact time and constant orientation. The measurements are presented analytically in Table 10 and Table 11.

Μεταπτυχιακή Διπλωματική Εργασία, Αριστείδης Ρεπούλιας, ΑΜ 0014

Table 10. Force tests for various pairs of woven fabrics[*].

	two identical COT100%		two identical COT66%-PES34%		two identical WOOL100%		COT66%-PES34% and WOOL100%	
	F_{max} (N)	V_{max} (V)	F_{max} (N)	V_{max} (V)	F_{max} (N)	V_{max} (V)	F_{max} (N)	V_{max} (V)
Test 1	0,92	0,12	0,80	0,16	1,06	0,16	1,11	0,16
Test 2	0,92	0,16	0,81	0,16	1,02	0,24	1,14	0,24
Test 3	0,83	0,12	0,83	0,16	1,04	0,24	1,18	0,16
Test 4	0,84	0,16	0,81	0,20	1,13	0,24	1,20	0,24
Test 5	0,83	0,12	0,80	0,16	1,20	0,16	1,08	0,24
Test 6	0,83	0,16	0,57	0,20	1,20	0,16	1,09	0,17
Test 7	0,83	0,12	0,57	0,16	1,16	0,24	1,08	0,24
Test 8	0,83	0,16	0,91	0,12	1,22	0,24	1,13	0,16
Test 9	0,83	0,12	0,91	0,16	0,93	0,24	1,08	0,24
Test 10	1,05	0,16	0,92	0,12	0,94	0,24	1,13	0,16

[*] Distance: 3mm / Contact time: 200ms

Table 11. Force tests for various pairs of woven fabrics[*].

	two identical PES100%		PES100% and WOOL100%		PES100% and COT66%-PES34%		PES100% and COT100%	
	F_{max} (N)	V_{max} (V)	F_{max} (N)	V_{max} (V)	F_{max} (N)	V_{max} (V)	F_{max} (N)	V_{max} (V)
Test 1	0,54	2,64	0,47	3,12	0,70	1,80	0,89	2,68
Test 2	0,49	2,52	0,49	3,20	0,71	1,80	0,20	1,92
Test 3	0,50	2,52	0,06	1,76	0,70	1,80	0,82	2,68
Test 4	0,85	3,28	0,05	1,52	0,39	1,60	0,70	2,56
Test 5	0,88	3,20	0,75	3,68	0,37	1,68	0,74	2,56
Test 6	0,82	3,20	0,78	3,68	0,41	1,68	0,10	1,76
Test 7	0,63	2,88	0,51	3,20	0,25	1,48	0,96	2,96
Test 8	0,69	2,88	0,06	1,60	0,28	1,52	0,08	1,68
Test 9	0,39	2,16	0,16	1,76	0,13	1,36	0,98	3,12
Test 10	0,37	2,08	0,22	2,08	0,11	1,12	0,72	2,64
Test 11	0,34	2,08	0,21	2,16	0,14	1,36	0,73	2,60
Test 12	0,32	2,00	0,04	1,28	0,60	1,84	0,73	2,64
Test 13	0,25	1,60	0,79	3,68	0,59	1,76	0,88	2,67
Test 14	0,30	1,92	0,59	3,52	0,67	1,88	0,93	2,86
Test 15	0,21	1,44	0,55	3,44	0,74	1,80	0,44	2,34
Test 16	0,20	1,28	0,54	3,36	0,86	2,08	0,42	2,30
Test 17	0,94	3,36	0,95	3,52	0,86	2,08	0,12	1,85
Test 18	0,95	3,36	0,98	3,60	0,80	2,04	0,32	2,11
Test 19	0,16	1,20	0,94	3,52	0,78	2,00	0,63	2,56
Test 20	0,15	1,28	0,97	3,52	0,75	2,00	0,68	2,64

[*] Distance: 3mm / Contact time: 200ms

Μεταπτυχιακή Διπλωματική Εργασία, Αριστείδης Ρεπούλιας, ΑΜ 0014

In the beginning, the following pairs of textile fabrics were selected: two identical samples of COT100%, two identical samples of COT66%-PES34%, two identical samples of WOOL100%, two identical samples of PES100%, and COT66%-PES34% with WOOL100%. Because these sample pairs showed negligible voltage output, few measurements were carried out, except for PES100%. Secondly, pairs of different textile fabrics were selected: COT66%-PES34% with WOOL100%, PES100% with WOOL100%, PES100% with COT66%-PES34%, and PES100% with COT100%.

18.3. Test results for different duration of contact of the samples

To study contact's time duration between samples surfaces, one of the two samples tapped on the other one once, with various contact times but constant force and orientation.

The following pairs of textile fabrics were selected: two identical samples of PES100%, PES100% with WOOL100%, PES100% with COT66%-PES34% and PES100% with COT100%. The measurements are presented analytically from Table 12 to Table 15.

Table 12. Contact time test for two identical PES100% woven fabrics*.

Contact time	80 ms	200 ms	500 ms
	V_{max} (V)	V_{max} (V)	V_{max} (V)
Test 1	3.44	3.44	3.52
Test 2	3.44	3.52	3.44
Test 3	3.44	3.52	3.36
Test 4	3.52	3.36	3.36
Test 5	3.44	3.36	3.52
Average	3.46	3.44	3.44
STD	0.04	0.08	0.08
CV	1.04	2.33	2.33

* Distance: 3mm

Table 13. Contact time test for PES100% and WOOL100% woven fabrics*.

Contact time	80 ms	200 ms	500 ms
	V_{max} (V)	V_{max} (V)	V_{max} (V)
Test 1	3.52	3.52	3.52
Test 2	3.52	3.44	3.60
Test 3	3.52	3.44	3.52
Test 4	3.36	3.36	3.52
Test 5	3.44	3.44	3.52
Average	3.47	3.44	3.54
STD	0.07	0.06	0.04
CV	2.06	1.64	1.01

* Distance: 3mm

Table 14. Contact time test for PES100% and COT66%-PES34% woven fabrics*.

Contact time	80 ms	200 ms	500 ms
	V_{max} (V)	V_{max} (V)	V_{max} (V)
Test 1	2.04	2.00	2.00
Test 2	2.00	2.08	2.00
Test 3	2.00	2.04	2.00
Test 4	2.00	1.92	2.00
Test 5	2.12	2.00	1.96
Average	2.03	2.01	1.99
STD	0.05	0.06	0.02
CV	2.57	2.95	0.90

* Distance: 3mm

Table 15. Contact time test for PES100% and COT100% woven fabrics*.

Contact time	80 ms	200 ms	500 ms
	V_{max} (V)	V_{max} (V)	V_{max} (V)
Test 1	2.64	2.64	2.64
Test 2	2.64	2.64	2.64
Test 3	2.72	2.72	2.64
Test 4	2.68	2.64	2.60
Test 5	2.72	2.68	2.64
Average	2.68	2.66	2.63
STD	0.04	0.04	0.02
CV	1.49	1.34	0.68

* Distance: 3mm

18.4. Test results for different surface patterns of textile samples

In these tests, two woven textile fabrics having a different surface pattern on each of their sides were examined: one velvet and one wafer. These were both COT100% made. In each test, one fabric's side was paired and tested with a PES100% textile fabric in the testing device. The PES100% fabric sample was selected in order to cause adequate voltage outcomes. The contact time, surfaces orientation and contact force were constant. The recorded measurements are presented below in Table 16 and Table 17.

Table 16. Surface pattern test for the COT100% (wafer) and PES100% woven fabrics*.

	Side A		Side B	
	F_{max} (N)	V_{max} (V)	F_{max} (N)	V_{max} (V)
Test 1	0,65	2,32	0,64	1,68
Test 2	0,65	2,24	0,63	1,76
Test 3	0,66	2,36	0,64	1,76
Test 4	0,64	2,32	0,62	1,68
Test 5	0,64	2,28	0,64	1,76
Test 6	0,64	2,32	0,63	1,68
Test 7	0,62	2,32	0,64	1,84
Test 8	0,65	2,32	0,64	1,84
Test 9	0,63	2,40	0,64	1,84
Test 10	0,64	2,32	0,66	1,88
Average	**0,64**	**2,32**	**0,64**	**1,77**
STD	0,01	0,04	0,01	0,08
CV	1,74	1,82	1,59	4,26

* Distance: 3mm / Contact time: 200ms

Table 17. Surface pattern test for COT100% (Velvet) and PES100% woven fabrics*.

	Pile side		Plain side	
	F_{max} (N)	V_{max} (V)	F_{max} (N)	V_{max} (V)
Test 1	1,02	4,48	1,06	2,80
Test 2	1,00	4,48	1,06	2,80
Test 3	0,98	4,48	1,07	2,80
Test 4	0,91	4,48	1,07	2,80
Test 5	0,98	4,48	1,02	2,96
Test 6	0,93	4,48	1,00	2,72
Test 7	1,01	4,48	1,02	2,88
Test 8	0,96	4,64	1,01	2,88
Test 9	1,01	4,32	0,93	2,80
Test 10	1,00	4,48	0,97	2,88
Average	**0,98**	**4,48**	**1,02**	**2,83**
STD	0,04	0,08	0,05	0,07
CV	3,65	1,68	4,45	2,38

* Distance: 3mm / Contact time: 200ms

19. Analysis of results

19.1. Analysis of results for different orientations of the samples surfaces during contact

It was found that by tapping the fabrics of COT100%, COT 66%-PES 34% or WOOL100%, no matter if the samples pairs were identical or different, the created voltage is insignificant. Average V_{max} was measured 0,15-0,21V. So any possible effect of their surfaces orientation at the moment of the contact could not be detected. Tests were also made by pairing COT100% with COT66%-PES34%, and COT100% with WOOL100%, but their measurements were not presented analytically in the previous chapter as their voltage outputs are negligible too.

On the other hand, we noticed that tapping the PES100% sample with an identical one or with any of the other available samples (COT100%, COT66%-PES34% or WOOL100%), created electric outcomes (Table 18). Average V_{max} was measured 1,84-3,53V.

The pair of WOOL100% with PES100% gave higher voltages than the rest of the tests. This can be justified by the materials position in the triboelectric series table and the rough surface of the WOOL100% fabric, which intensifies the mechanisms of triboelectricity.

Table 18. Average V_{max} values for each orientation and each pair of woven fabrics*.

Sample 1	Sample 2	Average V_{max} at each angle (V)			
		$0°$	$-90°$	$90°$	$180°$
COT 100%	COT 100%	0.17	0.16	0.16	0.15
COT 66%-PES 34%	COT 66%-PES 34%	0.17	0.15	0.15	0.17
WOOL 100%	WOOL 100%	0.21	0.21	0.19	0.21
COT 66%-PES 34%	WOOL 100%	0.21	0.19	0.21	0.21
COT 100%	COT 66%-PES 34%	0.17	0.17	0.16	0.17
COT 100%	WOOL 100%	0.18	0.18	0.17	0.17
PES 100%	PES 100%	3.38	3.26	3.28	3.39
PES 100%	WOOL 100%	3.52	3.42	3.39	3.53
PES 100%	COT 66%-PES 34%	2.00	1.84	1.86	1.99
PES 100%	COT 100%	2.63	2.61	2.62	2.65

*Distance: 3mm / Contact time: 200ms

All the samples which were used were woven textile fabrics, thus having a warp and weft direction. So, concerning the orientation of the warps or wefts of the paired samples at the moment of the contact, the measurements do not differ significantly. Though for

Μεταπτυχιακή Διπλωματική Εργασία, Αριστείδης Ρεπούλιας, ΑΜ 0014

the PES100% with PES100%, PES100% with WOOL100% and PES100% with COT66%-PES34% pairs of samples, a small difference is noticed when comparing the voltages measured at reverse orientations 0° or 180° with the ones measured at -90° or 90° (Figure 57). So the rotation of one sample at 0° and 180° in relation to the other sample (or at -90° and 90° respectively) gives similar surface contact which equals to similar voltage output.

A possible explanation for such a tendency can be the different forms of the fabrics surfaces if examining it on a micro-scale. The structural elements of each woven fabric (warps and wefts) are creating concave and convex tiny areas upon their overlap on their surface, so that these areas can match and osculate more or less, depending on the weaving pattern, the fibres thickness, the roughness of the surface etc of the fabrics.
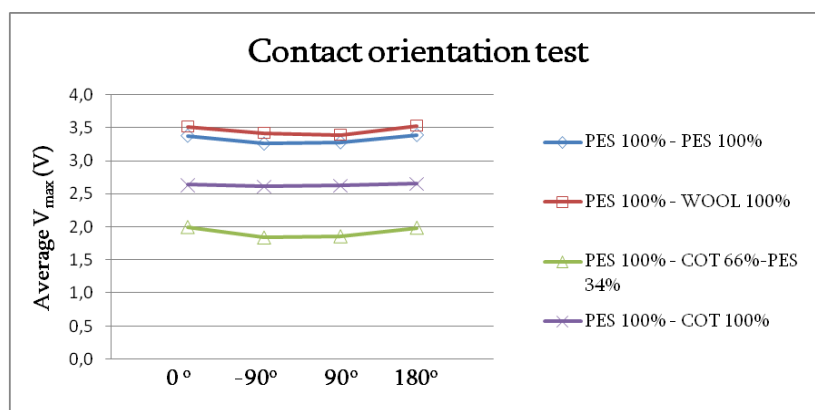
Figure 57. Graph of average V_{max} values for each orientation and each pair of samples.

This notification might become more clear to be answered if future tests will be applied with textile fabrics of more intensively different surface patterns along the warp and weft direction, thus driving to more intensive results at contacts of various orientations.

19.2. Analysis of results for different contact forces between the samples surfaces

In the case of the COT100%, COT 66%-PES 34% or WOOL100% fabrics, no matter if the samples pairs were identical or different, the created voltage was insignificant no matter the intensity of the applied force. The same result appeared for the tests made by pairing COT100% with COT66%-PES34%, and COT100% with WOOL100%, whose measurements were not presented analytically in the previous chapter as their voltage outputs are negligible too.

Regarding the results of the rest of the pairs of samples, in Figure 58 we can see an increase of V_{max} values when contact force increases. The pair of PES100% with WOOL100% gave the highest voltages again as before.

Unfortunately, the force applied by the solenoid of the tapping system is limited, thus not permitting to examine the electrical outputs of the samples contact under higher contact force.

The increase of the voltage upon the increase of the applied contact force agrees with the theory, which indicates that if two surfaces contact better each other, then their effective contact area rises and the electrical outputs increase.
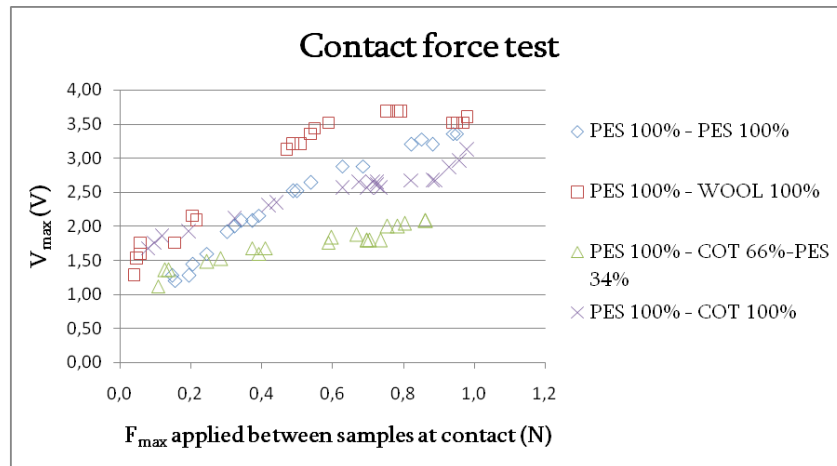
Figure 58. Graph of the V_{max} values for various forces and various pairs of samples.

19.3. Analysis of results for different contact time durations between the samples

On the selected pairs of samples, the results showed no significant difference between the maximum output voltages measured at 80ms, 200ms and 500ms contact time durations, for a single contact and separation execution. Thus it seems that the contact duration does not affect the selected samples output voltage, which agrees with the theory mentioning that the phenomenon happens only instantly at the moment of the contact and is independent of the time. The average values of V_{max} are presented in Table 19.

Table 19. Average V_{max} values for each contact time and each pair of woven fabrics[*].

	Contact time		
	80 ms	200 ms	500 ms
Samples of woven fabrics	Average V_{max} (V)		
two identical PES100%	3.46	3.44	3.44
PES100% and WOOL100%	3.47	3.44	3.54
PES100% and COT66%-PES34%	2.03	2.01	1.99
PES100% and COT100%	2.68	2.66	2.63

[*] Distance: 3mm

19.4. Analysis of results for different surface patterns of textile samples

In these tests, the contact force, contact orientation and contact time were constant, while the samples with two different sides were reversed consecutively.

The COT100% wafer fabric showed a significant voltage increase on side A when tapped with the PES100% fabric (Table 20). Here we must mention that side A is the one

Μεταπτυχιακή Διπλωματική Εργασία, Αριστείδης Ρεπούλιας, ΑΜ 0014

with the look of waffle-like squares (characteristic of the wafer pattern design) thus providing a more effective area to achieve better contact with the PES100% fabric, and higher voltage outcome. On the other hand, side B which could provide less effective area because of its weaving pattern gave lower electrical outcomes.

Table 20. Average V_{max} values for each orientation and each pair of woven fabrics[*].

Sample 1	Sample 2	V_{max} (V)	Stand. Dev.
PES 100%	COT100% wafer - side A	2.32	0.04
PES 100%	COT100% wafer - side B	1.77	0.08

[*] Distance: 3mm / Contact time: 200ms

A similar result came from the test of the COT100% velvet fabric with the PES100% fabric. The side with the pile finishing which gives the velvet look, gave significantly higher voltage when tapped with the PES100% sample Table 21. On the other hand, the plain side gave a lower voltage when tapped with the PES100% sample. Again as in the previous case, the higher effective area of the pile side drove to a higher output voltage.

Table 21. Average V_{max} values for each orientation and each pair of woven fabrics[*].

Sample 1	Sample 2	V_{max} (V)	Stand. Dev.
PES 100%	COT100% velvet - pile side	4.48	0.08
PES 100%	COT100% velvet - plain side	2.83	0.07

[*] Distance: 3mm / Contact time: 200ms

Through this test, it became clear how important the surface pattern of a textile fabric can be for its triboelectric outcomes. It also seemed that the developed prototype testing device can help a lot in comparing the triboelectric outcomes of different fabrics.

Μεταπτυχιακή Διπλωματική Εργασία, Αριστείδης Ρεπούλιας, ΑΜ 0014

20. Conclusions of tests

Concerning the developed prototype testing device, it was really useful in comparing the triboelectric outcomes of different textile fabric samples under the same testing conditions. The following parameters were controllable throughout the tests: contact time, contact force, contact orientation, contact materials. We must mention that its tests showed satisfying repeatability and constant precision on the measurements.

As a first conclusion, we saw that even natural material fabrics can give electrical outputs when combined with a synthetic one, no matter if they have not been coated with conductive materials. More specifically, the COT100%, COT 66%-PES 34% or WOOL100% fabric samples did not create any significant electrical outputs when tapped together in identical or combined pairs, but tapping them with PES100% fabric, the phenomenon became more intensive, giving significant voltage outputs. This follows the triboelectric series theory, where the longer the distance between the positions of the selected materials in the triboelectric series table, the more intensive will be the phenomenon.

The rough surface of the WOOL100% when combined with the PES100% offered high effective area, and thus high voltage, which agreed with the relevant theory. Moreover, its position in the triboelectric series table strengthens the creation of high voltage. Thus both the material and the structure played a significant role in the electric outcomes.

Moreover, we verified the paradox of creating voltage when tapping identical materials [8]. These were two identical PES100% textile fabric samples. Although the triboelectric series theory does not anticipate the triboelectric phenomenon [1,5] however voltage was created following the theories of ions transfer and material transfer.

The orientation of the samples surfaces at four opposite different possible angles, at the moment of the contact, seemed to be insignificant. Though for the PES100% with PES100%, PES100% with WOOL100% and PES100% with COT66%-PES34% pairs of samples, a small difference is noticed when comparing the voltages measured at reverse orientations 0° or 180° with the ones measured at -90° or 90°. So the rotation of one sample at 0° and 180° in relation to the other sample (or at -90° and 90° respectively) gives similar surface contact which equals to similar voltage output. If this is true, a possible explanation for such a tendency can be the different forms of the fabrics surfaces if examining it on a micro-scale. We must keep in mind that the structural elements of each woven fabric (warps and wefts) are creating concave and convex tiny areas upon their overlap on their surface, so that these areas can match and osculate more or less, depending on the weaving pattern, the fibres thickness, the roughness of the surface etc of the fabrics.

There is also a clear increase of the V_{max} values with the increase of the contact force, concerning the pairs of samples which create voltages in this study. Different pairs of samples have shown different increasing curves. This notification agrees with the case of a bending contact-separation mode TEG developed by Fan et al. where increasing the applied strain resulted in increasing of the electrical output current due to better contact between the surfaces [10], and the case of a contact-separation mode TEG built by Dudem et al. where the compression force increased also the electrical outputs [17].

The contact duration seemed not to affect the electric outcomes for a single contact and separation action. More specifically, when using the selected pairs of samples with the PES100% sample, the created output voltages had no significant difference between the 80ms, 200ms or 500ms contact time durations. This notification agrees with the findings of Baytekin et al. where Kelvin Force Microscopy (KFM) was used to verify that the phenomenon seems to be independent of the surfaces contact time for longer time durations [5].

Concerning the surface form of the textile fabric samples used, through the simple tests of two fabrics with different surface forms on their sides, it seemed that it can affect significantly the triboelectric outcomes, as they offer different effective contact areas following the theory [46]. In the case of the wafer fabric tested with the PES100% fabric, it was found that the side with the waffle shaped surface (small squares) created higher voltages, probably due to its higher effective area when contacting to the PES100% fabric. This agrees with Logothetis et al. who measured the generated voltage on samples of different surface areas and showed that increasing the contact area increases the voltage outputs too [18]. Moreover, in the case of the velvet fabric tested with the PES100% fabric, it was found that the side with the piled surface gave higher voltage than the plain side, probably due to the higher effective contact area. This agrees with previous theories which mention that high roughness of contacting surfaces affects TEGs electrical outputs [3] by increasing their effective area of friction [21].

The next step for future work seems to be the study of the triboelectricity phenomenon on a wider selection of more effective textile fabric structures, which will be classified according to their thickness, density, conductivity, weaving or knitting pattern, roughness, finishings etc.

21. General conclusion
In the past, the use of textiles was primarily focused on structural and aesthetic applications, like fashion, decoration, protection and insulation [64]. In each application, the functionality of textiles was defined only by the raw material (fibres) properties and by the techniques used to bind fibres into fabrics (directly in the case of non-wovens or after forming yarns for wovens and knitted fabrics).

Over the last decades, we have seen a rapid development of portable devices and the big market they share have created a big challenge for the areas of textile technology and

electronics to work closely and cover the coming demands of new wearable applications [65].

Textiles are considered very promising to achieve this goal as due to their properties they are ideal for creating or supporting flexible, multifunctional wearable electronics. The physical binding of fibres or yarns forms textile structures, which combine human-friendly properties like conformability, excellent skin contact and breathability, with significant structural properties like tensile recovery and shear strength [64]. Moreover, being generally lightweight, flexible [66] and characterised by easy fabrication, various designs and low-cost production, they have become the most versatile materials found today [65].

A final conclusion that emerges from this study is that triboelectricity may include cleavage of bonds, chemical changes, or transfer of material, ions or electrons or their combinations [5]. So triboelectricity seems to be a complex phenomenon which requires input from several scientific disciplines to be completely understood [1].

It has been observed that numerous scientists have built TEGs focusing mostly to reach higher voltage and current outputs than to study or relate materials and surface patterns under controllable external conditions (e.g. contact time, contact force etc). Keeping in mind the absence of a standard device, plus the requirement of making repeatable and reliable measurements, the design and construction of the current prototype testing device where textile fabric samples will be inserted and tested under the same conditions seemed to be really effective and interesting, and we hope it will help in the progress of understanding the triboelectricity phenomenon.

Μεταπτυχιακή Διπλωματική Εργασία, Αριστείδης Ρεπούλιας, ΑΜ 0014

BIBLIOGRAPHY

[1]   Williams M W 2017 What Creates Static Electricity? *Am. Sci.* **100** 316–23

[2]   Williams M W 2012 Triboelectric charging of insulating polymers–some new perspectives *AIP Adv.* **2**

[3]   Molnar A, Gerasimov V and Piotr Kurytnik I 2018 Triboelectricity and construction of power generators based on it *Przegląd Elektrotechniczny* **1** 167–71

[4]   Lin Z, Chen J and Yang J 2016 Recent Progress in Triboelectric Nanogenerators as a Renewable and Sustainable Power Source *J. Nanomater.* **2016** 1–24

[5]   Baytekin H, Patashinski A, Branicki M, Baytekin B, Soh S and Grzybowski B 2011 The Mosaic of Surface Charge in Contact Electrification *Science* **333** 308–12

[6]   F. Diaz A and M. Felix-Navarro R 2004 A Semi-Quantitative Tribo-Electric Series for Polymeric Materials: The Influence of Chemical Structure and Properties *J. Electrost.* **62** 277–90

[7]   Anon 2019 Hindenburg disaster *Wikipedia*

[8]   J Lacks D and Mohan Sankaran R 2011 Contact electrification of insulating materials *J. Phys. Appl. Phys.* **44** 453001

[9]   Mallineni S S K, Behlow H, Podila R and M. Rao A 2017 A low-cost approach for measuring electrical load currents in triboelectric nanogenerators *Nanotechnol. Rev.*

[10]   Fan F, Tian Z-Q and Wang Z 2012 Flexible triboelectric generator *Nano Energy* **1** 328–334

[11]   Chacko P, S Kapildas K and T J 2017 Nano Generator Intended for Energy Harvesting *Asian J. Appl. Sci. Technol. AJAST* **1** 88–91

[12]   Gowrishankar R 2017 Constructing triboelectric textiles with weaving ISWC '17 pp 170–1

[13]   Paosangthong W, Torah R and Beeby S 2018 Recent Progress on Textile-Based Triboelectric Nanogenerators *Nano Energy* **55**

[14]   Zhong J, Zhang Y, Zhong Q, Qiyi hu, Hu B, Wang Z and Zhou J 2014 Fiber-Based Generator for Wearable Electronics and Mobile Medication *ACS Nano* **8**

Μεταπτυχιακή Διπλωματική Εργασία, Αριστείδης Ρεπούλιας, ΑΜ 0014

[15] Li C, Cao R and Zhang X 2018 Breathable Materials for Triboelectric Effect-Based Wearable Electronics *Appl. Sci.* **8** 2485

[16] Bhatnagar V and Owende P 2015 Energy Harvesting for Assistive and Mobile Applications *Energy Sci. Eng.* **3**

[17] Dudem B, Mule A, Patnam H and Su Yu J 2018 Wearable and durable triboelectric nanogenerators via polyaniline coated cotton textiles as a movement sensor and self-powered system *Nano Energy* **55**

[18] Logothetis I, Vassiliadis S and Siores E 2017 Triboelectric effect in energy harvesting *IOP Conf. Ser. Mater. Sci. Eng.* **254** 042021

[19] Hu Y and Zheng Z 2018 Progress in textile-based triboelectric nanogenerators for smart fabrics *Nano Energy* **56**

[20] Yu A, Pu X, Wen R, Liu M, Zhou T, Zhang K, Zhang Y, Zhai J, Hu W and Wang Z 2017 Core-Shell-Yarn-Based Triboelectric Nanogenerator Textiles as Power Cloths *ACS Nano* **11**

[21] Zhang X-S, Han M-D, Meng B and Zhang H-X 2014 High performance triboelectric nanogenerators based on large-scale mass-fabrication technologies *Nano Energy* **11**

[22] Mahmud M A, Huda N, Farjana S, Asadnia M and Lang C 2017 Recent Advances in Nanogenerator-Driven Self-Powered Implantable Biomedical Devices *Adv. Energy Mater.* **8** 1701210

[23] Musa U G, Doruk Cezan S, Baytekin B and Baytekin H 2018 The Charging Events in Contact-Separation Electrification *Sci. Rep.* **8**

[24] Mahaut G 2019 *Triboelectricity* (Department of Electrical and Electronics Engineering, University of West Attica, Athens, Greece - Ecole Nationale Supérieure des Arts et Industries Textiles, Roubaix, France)

[25] Pan S and Zhang Z 2018 Fundamental theories and basic principles of triboelectric effect: A review *Friction* **7**

[26] V. Gitis N 2001 Electrophysical Phenomena in the Tribology of Polymers *Chem. Eng. J. - CHEM ENG J* **83** 65–6

[27] Williams M W 2011 Mechanisms of Triboelectric Charging of Insulators, a Coherent Scenario *Proc. ESA Annual Meeting on Electrostatics 2011* ESA Annual Meeting on Electrostatics

Μεταπτυχιακή Διπλωματική Εργασία, Αριστείδης Ρεπούλιας, ΑΜ 0014

[28]   Wang Z and Song J 2006 Piezoelectric Nanogenerators Based on Zinc Oxide Nanowire Arrays *Science* **312** 242–6

[29]   Li X, Tao J, Zhu J and Pan C 2017 A nanowire based triboelectric nanogenerator for harvesting water wave energy and its applications *APL Mater.* **5** 074104

[30]   Wang S, Lin L and Wang Z 2012 Nanoscale Triboelectric-Effect-Enabled Energy Conversion for Sustainably Powering Portable Electronics *Nano Lett.* **12**

[31]   Wang S, Lin L, Xie Y, Jing Q, Niu S and Wang Z 2013 Sliding-Triboelectric Nanogenerators Based on In-Plane Charge-Separation Mechanism *Nano Lett.* **13**

[32]   Yang Y, Sheng Zhou Y, Zhang H, Liu Y, Lee S and Wang Z 2013 A Single-Electrode Based Triboelectric Nanogenerator as Self-Powered Tracking System *Adv. Mater. Deerfield Beach Fla* **25**

[33]   Wang S, Xie Y, Niu S, Lin L and Wang Z 2014 Freestanding Triboelectric-Layer Based Nanogenerators for Harvesting Energy from a Moving Object or Human Motion in Contact and Non-Contact Modes. *Adv. Mater. Deerfield Beach Fla* **26**

[34]   Zhang H, Jiwei Z, Hu Z, Quan L, Shi L, Chen J, Peng X, Zhang Z, Dong S and Luo J 2019 Waist-wearable wireless respiration sensor based on triboelectric effect *Nano Energy* **59**

[35]   Mallineni S S K, Behlow H, Dong Y, Bhattacharya S, M. Rao A and Podila R 2017 Facile and robust triboelectric nanogenerators assembled using off-the-shelf materials *Nano Energy* **35** 263–70

[36]   Hu Y, Zhao Z and Liu Z 2018 Textile triboelectric nanogenerator for wearable electronics *Adv. Mater. Lett.* **9** 199–204

[37]   Yin Y, Wang J, Zhao S, Fan W, Zhang X, Zhang C, Xing Y and Li C 2018 Stretchable and Tailorable Triboelectric Nanogenerator Constructed by Nanofibrous Membrane for Energy Harvesting and Self-Powered Biomechanical Monitoring *Adv. Mater. Technol.* **3** 1700370

[38]   Zhou T, Zhang C, Han C, Fan F, Tang W and Wang Z 2014 Woven Structured Triboelectric Nanogenerator for Wearable Devices *ACS Appl. Mater. Interfaces* **6**

[39]   Li H, Zhao S, Du X, Wang J, Cao R, Xing Y and Li C 2018 A Compound Yarn Based Wearable Triboelectric Nanogenerator for Self-Powered Wearable Electronics *Adv. Mater. Technol.* **3**

Μεταπτυχιακή Διπλωματική Εργασία, Αριστείδης Ρεπούλιας, ΑΜ 0014

[40] Jung W-S, Kang M-G, Moon H G, Baek S-H, Yoon S-J, Wang Z, Kim S-W and Kang C-Y 2015 High Output Piezo/Triboelectric Hybrid Generator *Sci. Rep.* **5** 9309

[41] Xu C, Zhang B, Chi Wang A, Zou H, Liu G, Ding W, Wu C, Ma M, Feng P, Lin Z and Wang Z 2019 Contact-Electrification Between Two Identical Materials: Curvature Effect *ACS Nano* **13**

[42] Sun H, Chu H, Wang J, Ding L and Li Y 2010 Kelvin probe force microscopy study on nanotriboelectrification *Appl. Phys. Lett.* **96** 083112–083112

[43] Yeong Kim D, Soo Kim H and Jung J 2016 Ar plasma treated polytetrafluoroethylene films for a highly efficient triboelectric generator *J. Korean Phys. Soc.* **69** 1720–3

[44] Kwak S S, Kim H, Seung W, Kim J, Hinchet R and Kim S-W 2017 Fully Stretchable Textile Triboelectric Nanogenerator with Knitted Fabric Structures *ACS Nano* **11**

[45] Pham R, Virnelson R, Mohan Sankaran R and J. Lacks D 2011 Contact charging between surfaces of identical insulating materials in asymmetric geometries *J. Electrost.* **69** 456–60

[46] Huang T, Zhang J, Yu B, Yu H, Long H, Wang H, Zhang Q and Zhu M 2019 Fabric texture design for boosting the performance of a knitted washable textile triboelectric nanogenerator as wearable power *Nano Energy* **58**

[47] Zhu G, Su Y, Bai P, Chen J, Jing Q, Yang W and Wang Z 2014 Harvesting Water Wave Energy by Asymmetric Screening of Electrostatic Charges on a Nanostructured Hydrophobic Thin-Film Surface *ACS Nano* **8**

[48] Liang Q, Yan X, Liao X and Zhang Y 2016 Integrated multi-unit transparent triboelectric nanogenerator harvesting rain power for driving electronics *Nano Energy* **25** 18–25

[49] Yong H, Chung J, Choi D, Jung D, Cho M and Lee S 2016 Highly reliable wind-rolling triboelectric nanogenerator operating in a wide wind speed range *Sci. Rep.* **6** 33977

[50] Zhang L, Zhang B, Chen J, Jin L, Deng W, Tang J, Zhang H, Pan H, Zhu M, Yang W and Lin Wang Z 2015 Lawn Structured Triboelectric Nanogenerators for Scavenging Sweeping Wind Energy on Rooftops *Adv. Mater. Deerfield Beach Fla* **28**

Μεταπτυχιακή Διπλωματική Εργασία, Αριστείδης Ρεπούλιας, ΑΜ 0014

[51] Wang Z, Ruan Z, Ng W, Li H, Tang Z, Liu Z, Wang Y, Hu H and Zhi C 2018 Integrating a Triboelectric Nanogenerator and a Zinc-Ion Battery on a Designed Flexible 3D Spacer Fabric *Small Methods* **2**

[52] Hou T-C, Yang Y, Zhang H, Chen J, Chen L-J and Lin Wang Z 2013 Triboelectric nanogenerator built inside shoe insole for harvesting walking energy *Nano Energy* **2** 856–62

[53] He T, Shi Q, Wang H, Wen F, Chen T, Ouyang J and Lee C 2018 Beyond Energy Harvesting - Multi-Functional Triboelectric Nanosensors on A Textile *Nano Energy* **57**

[54] Lin Z, Chen J, Li X, Zhou Z, Meng K, Wei W, Yang J and Lin Wang Z 2017 Triboelectric Nanogenerator Enabled Body Sensor Network for Self-Powered Human Heart-Rate Monitoring *ACS Nano* **11**

[55] Mao Y, Geng D, Er-Jun L and Wang X 2015 Single-Electrode Triboelectric Nanogenerator for Scavenging Friction Energy from Rolling Tires *Nano Energy* **15**

[56] Bertacchini A and Pavan P 2019 An Ultra-Low Cost Triboelectric Flowmeter *Applications in Electronics Pervading Industry, Environment and Society* pp 109–15

[57] Bai P, Zhu G, Liu Y, Chen J, Jing Q, Yang W, Ma J, Zhang G and Wang Z 2013 Cylindrical Rotating Triboelectric Nanogenerator *ACS Nano* **7**

[58] Kuang S, Chen J, Bei Cheng X, Zhu G and Lin Wang Z 2015 Two-dimensional rotary triboelectric nanogenerator as a portable and wearable power source for electronics *Nano Energy* **17**

[59] Feng Y, Huang X, Liu S, Guo W, Li Y and Wu H 2019 A self-powered smart safety belt enabled by triboelectric nanogenerators for driving status monitoring *Nano Energy* **62**

[60] Cao R, Wang J, Zhao S, Yang W, Yuan Z, Yin Y, Du X, Li N, Zhang X, Li X, Wang Z and Li C 2017 Self-powered nanofiber-based screen-print triboelectric sensors for respiratory monitoring *Nano Res.* **11**

[61] Kiaghadi A, Baima M, Gummeson J, Andrew T and Ganesan D 2018 Fabric as a Sensor: Towards Unobtrusive Sensing of Human Behavior with Triboelectric Textiles pp 199–210

[62] Ouyang H, Liu Z, Li N, Shi B, Zou Y, Xie F, Ma Y, Li Z, Li H, Qiang Z, Qu X, Fan Y, Lin Wang Z, Zhang H and Li Z 2019 Symbiotic cardiac pacemaker *Nat. Commun.* **10**

Μεταπτυχιακή Διπλωματική Εργασία, Αριστείδης Ρεπούλιας, ΑΜ 0014

[63] Wang M, Li W, Chen You C, Wang Q, Zeng X and Chen M 2017 Triboelectric nanogenerator based on 317L stainless steel and ethyl cellulose for biomedical applications *RSC Adv* **7** 6772–9

[64] Dias T and Ratnayake A 2015 Integration of micro-electronics with yarns for smart textiles *Electronic Textiles* (Elsevier) pp 109–116

[65] Sahito I and Khatri A 2017 Smart and Electronic Textiles

[66] D.J.Sanghvi College of Engineering, Gandhi D, Gadodia D, Kadam S and Narula H 2014 E-Textiles Technology *Int. J. Eng. Trends Technol.* **16** 373–376